Journal Article

End-to-End Power Models for 5G Radio Access Network Architectures with a Perspective on 6G

Doorgakant, B., Fowdur, T.P., and Akinsolu, M.O.

Article

End-to-End Power Models for 5G Radio Access Network Architectures with a Perspective on 6G

Bhuvaneshwar Doorgakant [1], Tulsi Pawan Fowdur [1] and Mobayode O. Akinsolu [2],*

[1] Department of Electrical and Electronic Engineering, University of Mauritius, Réduit 80837, Mauritius; bhuvaneshwar.doorgakant3@umail.uom.ac.mu (B.D.); p.fowdur@uom.ac.mu (T.P.F.)
[2] Faculty of Arts, Computing and Engineering, Wrexham University, Wrexham LL11 2AW, UK
* Correspondence: m.o.akinsolu@ieee.org or mobayode.akinsolu@wrexham.ac.uk

Abstract: 5G, the fifth-generation mobile network, is predicted to significantly increase the traditional trajectory of energy consumption. It now uses four times as much energy as 4G, the fourth-generation mobile network. As a result, compared to previous generations, 5G's increased cell density makes energy efficiency a top priority. The objective of this paper is to formulate end-to-end power consumption models for three different 5G radio access network (RAN) deployment architectures, namely the 5G distributed RAN, the 5G centralized RAN with dedicated hardware and the 5G Cloud Centralized-RAN. The end-to-end modelling of the power consumption of a complete 5G system is obtained by combining the power models of individual components such as the base station, the core network, front-haul, mid-haul and backhaul links, as applicable for the different architectures. The authors considered the deployment of software-defined networking (SDN) at the 5G Core network and gigabit passive optical network as access technology for the backhaul network. This study examines the end-to-end power consumption of 5G networks across various architectures, focusing on key dependent parameters. The findings indicate that the 5G distributed RAN scenario has the highest power consumption among the three models evaluated. In comparison, the centralized 5G and 5G Cloud C-RAN scenarios consume 12% and 20% less power, respectively, than the Centralized RAN solution. Additionally, calculations reveal that base stations account for 74% to 78% of the total power consumption in 5G networks. These insights helped pioneer the calculation of the end-to-end power requirements of different 5G network architectures, forming a solid foundation for their sustainable implementation. Furthermore, this study lays the groundwork for extending power modeling to future 6G networks.

Keywords: 5G; 6G; base station; energy efficiency; power models; RAN architectures; SDN

MSC: 68U01

1. Introduction

The excitement surrounding 5G and 6G technologies has been stoked by promising features including a historically high data throughput of 20 Gbps and a low latency of 1 millisecond [1]. According to recent projections [2], there may be up to 100 billion connected devices by 2030, and 5G networks may be able to handle data that is up to 1000 times better than 4G. However, there is a price to pay for the improvements in 5G and 6G networks. The primary constraint for 5G/6G systems is energy efficiency. According to [3], if energy-efficient installations are not taken into consideration, 5G networks run the

danger of using 140% more energy than a 4G network with a comparable coverage area. The primary cause of this increased power consumption is the higher density of base stations (BSs), antennas, cloud infrastructure, and user devices. According to [4], it is essential to prioritize energy efficiency and develop new strategies that address the entire network holistically. This includes planning, deployment management, and optimization to support the growing number of 5G connections and their stringent requirements.

A detailed analysis of mobile network power consumption by [5] revealed that BSs account for approximately 57% of the total network power usage. Additionally, [6] highlighted that power amplifiers contribute between 50% and 80% of the power consumption within BSs. Moreover, [5] highlighted that the BS, which includes the radio access network (RAN), is the most energy-intensive component of a mobile network. Mobile switching and the core network come in second and third, respectively. According to the International Telecommunications Union (ITU), energy efficiency is now one of 5G's primary competencies because of the considerations [7].

There are a number of gaps in the body of knowledge about 5G networks' power consumption. The majority of studies have concentrated on the amount of power used in a single 5G network section. For example, different models of power consumption for 5G BSs and mid-haul links based on mMIMO (massive multiple-input multiple-output) were examined by [4,8,9]. Ref. [10] developed models for the power usage in virtualized RAN settings, offering an alternative viewpoint. By concentrating on software-defined networking (SDN) technology, [11–14] investigated various strategies to optimize energy consumption at the core network level. However, [15] compared various backhaul communication architectures based on their power consumption models. On the other hand, the authors are unaware of any previous studies that have attempted to calculate the end-to-end power consumption of 5G networks by aggregating the power consumption at various 5G network segments. Also, much of the previous research has only looked at one or two particular 5G network topologies. Therefore, studies comparing the end-to-end power consumption of various 5G network topologies, both centralized and decentralized, are currently lacking.

This paper seeks to fill the aforementioned knowledge gap by delving deeply into the topic of 5G mobile networks' power usage across all of their constituent parts. Some research has developed models of 5G network power usage (see Section 2 for details); however, these studies have often focused on a small subset of the network. To be more specific, no prior work has considered all aspects of 5G networks, from the radio access network (RAN) to the core network, in order to produce a comprehensive model of power usage. As a result, this study bridges these gaps using different 5G deployment architectures. Therefore, the primary contributions of this paper are as follows:

- The development of end-to-end power models for three types of 5G network configurations: 5G Distributed RAN with mMIMO technology, Centralized 5G RAN with the CU deployed on dedicated hardware (similar to 5G Cloud D-RAN), and 5G Cloud Centralized-RAN with virtualized Distribution and Control units.
- The formulation of new equations for the end-to-end power consumption model of the three different 5G network scenarios, incorporating components such as BSs with mMIMO technology, front-haul, mid-haul, backhaul links, and the core network.
- A comparative analysis of the end-to-end power consumption of the three types of 5G network configurations, using realistic power consumption figures for the various components.
- Insights into the RAN architectures of 6G and the potential application of the proposed 5G power models in future 6G RANs.

The experiments and simulations conducted revealed that the 5G decentralized scenario exhibited the highest energy consumption. In contrast, the centralized 5G RAN and

5G Cloud C-RAN scenarios consumed 9% and 15% less power, respectively, compared to the decentralized scenario. The study also demonstrated that BSs generally accounted for approximately 74% to 78% of the total power consumption in 5G networks.

The remainder of this paper is organized as follows: Section 2 reviews recent related works. Section 3 provides an overview of 5G networks and the end-to-end power models for the three different 5G architectures, derived by combining equations from various network levels. In Section 4, the three power models developed in Section 3 are further analyzed and discussed using typical scenarios to project real power consumption values based on the available power ratings of different 5G RAN components. A comprehensive comparative analysis is then performed based on the results obtained for the power consumption of the three models. Section 5 offers insights into the RAN architectures of 6G and introduces basic power consumption models. Concluding remarks are provided in Section 6.

2. Related Work

Recent publications have proposed various strategies for modeling the power consumption of mobile networks. In [4], equations for carrier aggregation and mMIMO power consumption models were derived from three primary 5G deployment scenarios, including the D-RAN. Additionally, [4] presented a power consumption model for virtualized base band units (BBUs) in a cloud node, considering the effects of the cooling system, workload dispatcher switch, and general-purpose CPUs. The total power consumption of the RANs was analyzed based on these split alternatives.

By leveraging ML, researchers have developed realistic power models for 5G multi-carrier BSs [8]. To construct these models, extensive data was collected and input into an ML algorithm designed to simulate the operation of 5G active antenna devices. The model was built and evaluated for accuracy using an artificial neural network (ANN).

The concept of virtualizing radio access networks (RANs) for 5G deployment has been explored in [10]. Significant advancements in network function virtualization (NFV) and software-defined networking (SDN) have enabled the virtualization of dual-site processing as an alternative to traditional baseband unit (BBU) methods. Additionally, the study analyzed the trade-off between mid-haul bandwidth requirements and power consumption across different functional splits. Specifically, it has been noted that the bandwidth affects the performance; hence, bandwidth requirements must be taken into consideration by network operators. On the other hand, power consumption is an important factor for optimizing the energy efficiency [10].

To achieve network scalability, enhanced flexibility, and cost reduction in the deployment of 5G/6G services, Ref. [11] focused on the application of network function virtualization (NFV) and software-defined networking (SDN) at the core network level. A controller managed all NFV and SDN control operations, and the core network's proposed energy-saving algorithm deactivated unnecessary network equipment and links based on their usage. Simulation results presented by [11] showed that the proposed algorithm could achieve energy savings of up to 70% compared to scenarios where all of the equipment and links remained constantly active. Moreover, the authors demonstrated that the proposed algorithm deployed in hybrid NFV and SDN scenarios realized energy savings of up to 90% of figures achieved by full NFV or SDN networks.

An assessment of the advantages of SDN over traditional networking was conducted by [12]. These advantages include enhanced flexibility in network management and the improved energy efficiency of core networks through optimized routing. Specifically, a strategy was proposed for categorizing SDN-based systems based on three primary characteristics: traffic awareness, end-system awareness, and rule placement. The work

carried out in [12] also emphasized the importance of balancing increased energy efficiency with maintaining necessary levels of network performance.

The framework proposed by [13] primarily focused on optimization strategies for traffic management and load balancing to enhance the energy efficiency of SDN. To achieve this, a sleep-active mode was implemented, and a heuristic approach was employed for route selection. The mathematical model derived in [13] for the energy consumption of SDN-based networks comprised three main components, namely switches, controllers, and active links, and also catered for the network latency. Specifically, two stacks of routing protocols are fed to the heuristic-based algorithms, which determine the protocol having the lowest controller and link energy consumption. Thus, the route selection exercise is optimized by minimizing the links' and network controllers' energy consumption. Thorough simulations were conducted on two main types of networks, classified according to the number of their sizes, in terms of nodes and traffic profiles according to the rate of traffic arrival. The first network type was comprised of a maximum of 50 nodes, 4 controllers, and 50 links, whereas the second network type included up to 150 nodes, 10 controllers, and 200 links. The performance of the heuristic-based algorithm was assessed in comparison with conventional routing protocols such as the routing information protocol (RIP) and open shortest path first (OSPF), using the traffic rates of the order of 1000 packets per second. The results demonstrated that the proposed optimization approach reduced the energy consumption for SDN traffic management and load balancing by up to 25%.

In [14], two models for the power consumption of 5G standalone networks and a novel routing technique for allocating BS load in scenarios requiring intercellular communication were developed. The study proposed solutions to evenly distribute connection loads among BSs, focusing on optimizing wireless communications between user equipment and the network, thereby maximizing the use of physical infrastructure. To enhance the accuracy of power consumption predictions, Ref. [14] introduced a second model incorporating a novel cooling technique for 5G BSs. This model implemented a new routing protocol that utilized shortest path algorithms with weights based on the BS's power consumption.

The power consumption of backhaul in heterogeneous mobile networks was comprehensively analyzed in [15]. The evaluation considered traffic levels and various technologies, including microwave and the gigabit passive optical network (GPON), within fiber-to-the-home (FTTH) scenarios. A detailed breakdown of all of the components required for different designs was provided.

Most prior studies, including those discussed earlier, have concentrated on the power consumption of individual network nodes. As outlined in Section 1, the primary aim of this study is to determine the end-to-end power consumption of three main types of 5G network architectures: 5G Distributed RAN (D-RAN) utilizing mMIMO technology, centralized 5G RAN with dedicated hardware for the central unit (CU), and 5G Cloud C-RAN, which is analogous to 5G Cloud D-RAN. Conversely, preliminary research has been conducted on power consumption models for 6G networks. For example, Ref. [16] proposed an innovative architecture for a 6G network based on a Fog RAN (F-RAN). By incorporating photonic components, Ref. [16] evaluated the performance of the proposed 6G architecture using three main criteria: delay, power consumption, and energy efficiency.

The research conducted by [17] proposes a Power over Fibre (PoF) pooling mechanism to enhance energy efficiency, acknowledging the lack of a standardized framework for 6G communications. The study emphasizes the more stringent requirements of 6G technology, such as higher peak throughput speeds, reduced latency, and an improved

energy efficiency compared to 5G. Consequently, [17] introduced algorithms to support PoF pooling, enabling energy-aware device control and resource allocation management.

Building upon the previous research works, this paper proposes methodologies for estimating the power consumption of different segments of 5G networks. The main novelty of this paper is the development of end-to-end power consumption models for three different RAN architectures of 5G. The paper culminates in offering some insights into future works by discussing the power consumption of future 6G networks.

3. Power Models for 5G RAN

The D-RAN design has traditionally been the standard for mobile wireless network deployments. In a D-RAN system, BS has its own backhaul connection to the mobile core network. In contrast, the C-RAN architecture relocates the digital baseband processing hardware, known as the BBU, from the BSs to a central location. This centralization allows multiple RRHs to be serviced with simplified radio frequency (RF) electronics. Centralized processing for RANs is gaining traction due to its commercial and technological advantages, with RAN transport rates expected to be nearly 15 times higher than those of 4G LTE (Long-Term Evolution) [18]. Specifically, the Third Generation Partnership Project (3GPP) introduced a new and flexible design for the 5G RAN in Release 15 [19]. This design divides the BS, also referred to as a gNodeB or gNB (next-generation NodeB), into three logical components: the centralized unit (CU), the distributed unit (DU), and the radio unit (RU) [19]. According to [19], these components can perform various functions within the 5G New Radio (NR) stack. The front-haul network plays a significant role in a flexible RAN deployment for the transition from the common public radio interface (CPRI) to the enhanced CPRI (eCPRI). This enhanced interface offers greater bandwidth efficiency and facilitates interoperability between devices from various manufacturers.

Moreover, Ref. [20] illustrated the three distinct functional units that constitute the RAN elements: CU, DU, and RU. In this configuration, the functions of the BBU are distributed among the CU, DU, and RU as follows: the CU hosts Layer 3 Radio Resource Control (RRC) and Layer 2 Packet Data Convergence Protocol (PDCP) non-real-time operations; the DU is responsible for Layer 2 Radio Link Control (RLC), Media Access Control (MAC), and higher-layer Physical (PHY) operations; and the RU handles Layer 3 radio processing and higher-layer PHY functions [20]. The connection between the RU and the DU is established through the front-haul-low layer (Front-haul-LL). Due to the requirement for low-latency transmission, the distance between the RU and the DU is typically limited to 150 to 200 microseconds [20]. The Common Public Radio Interface (CPRI) is the most widely used standard for transmitting baseband I/Q signals from the BS to the radio device. It is important to note the amplitudes of the in-phase signal ('I') and the quadrature signal ('Q') [21].

The CPRI is a highly effective and versatile I/Q data interface compatible with various communication protocols, including GSM and LTE. eCPRI, which succeeded CPRI, specifies the requirements for connecting the Remote Radio Unit (RRU) and the DU. It is utilized in 5G networks as well as LTE-Advanced and LTE-Advanced Pro networks [22]. The 5G front-haul is essential for enabling use cases such as Internet of Things (IoT) networks, ultra-reliable low-latency communications (uRLLC), massive machine-type communication (mMTC), and enhanced mobile broadband (eMBB) [23]. The F1 interface, also known as the front-haul-high layer (Fronthaul-HL), connects the DU and the CU. This interface is also referred to as the mid-haul interface. Unlike the Front-haul-LL interface, the F1 interface is not constrained by latency requirements. Consequently, the Fronthaul-HL allows for further centralization by linking a gNB-CU to a gNB-DU.

To enable independent software and hardware maintenance cycles, cloud RAN virtualizes the baseband. In a fully cloudified cloud RAN, virtualized DUs (vDUs) manage

real-time baseband operations, while virtualized CUs (vCUs) handle non-real-time baseband operations [24]. The traditional one-size-fits-all approach to designing radio networks is no longer sufficient. According to [25], virtualizing the RAN edge facilitates the development of innovative wireless solutions for both businesses and consumers. Cloud RAN supports rapid service deployment and monetization, on-demand capacity scalability, and an adherence to stringent latency requirements. Network slicing from the RAN to the core network is increasingly important, and a fully cloudified cloud RAN solution is crucial for this [26].

In the 5G D-RAN paradigm, all processing occurs at the cell site. Conversely, the 5G C-RAN paradigm involves on-premises processing for the DU and RU, while the CU's processing is managed by a cloud or specialized hardware. According to [20], the 5G-cloud C-RAN model positions the RU at the cell site, with DU and CU operations conducted in the cloud. However, this centralized scenario requires an interface, referred to as the fronthaul-low layer, to connect the RU to the remote DU. Similarly, the interconnection of the DU and CU requires the midhaul interface, which is sometimes also referred to as the fronthaul-high layer interface. These interfaces require a high transmission capacity of the order of 100 Gbps as well as a low latency for efficient communication. These add to the complexity of the network. This co-location of BBUs and RF components at cell sites in the D-RAN architecture, also known as conventional RAN, saves the need for such fronthaul and midhaul connections, thereby simplifying the network deployment. The autonomous operation of each cell in the 5G D-RAN model enhances resilience, as a failure at one cell site does not impact the others, ensuring continuous network functionality. However, 5G D-RAN architecture is less efficient in resource utilization because it does not allow resource pooling across cell sites. In contrast, 5G-cloud C-RAN and 5G C-RAN architectures offer a greater network flexibility and scalability. These designs enable mobile operators to optimize energy consumption by dynamically allocating resources based on customer demand, leveraging shared processing capabilities across multiple cell sites. Centralizing equipment also reduces operational costs by simplifying network maintenance. Nonetheless, as noted by [26], the effectiveness of the cloud C-RAN model hinges on high-capacity, low-latency front-haul links between the RU and DU.

3.1. End-to-End Power Consumption Model for 5G D-RAN with mMIMO

The power model formulated for the 5G D-RAN scenario assumes that the network power consumption can be estimated by focusing solely on the power usage of the BS [4]. According to [4], the power consumption of a non-massive MIMO (non-mMIMO) BS is determined by the power usage of all its active antennas. Each antenna comprises a power amplifier, a radio frequency transceiver module, a BBU, a DC-DC power supply, and a cooling mechanism. Consequently, in this context, the components considered for end-to-end power consumption, as depicted in Figure 1, include PW_{BS} (the BS power consumption), PW_{SDN} (the Core Network power consumption), and PW_{BL} (the Backhaul network power consumption). Figure 1 illustrates the composition of the BS, comprising the RU and BBU unit situated in the same physical location. The BS is connected to the core network node in a centralized location via the backhaul links.
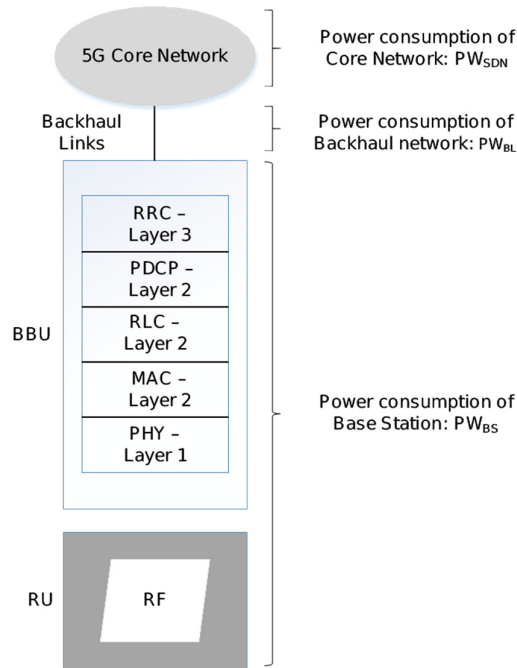
Figure 1. 5G D-RAN end-to-end power consumption model.

3.1.1. MIMO BS Power Consumption (PW_BS)

The BS is crucial in the 5G network as it provides wireless coverage to endpoints. After receiving digital packets from the main network, the gNodeB BSs convert them into radio signals. In 5G architecture, the BS redefines the BBU, RRU, feeder, and antenna into the CU and DU, with the RRU and antenna merging into the active antenna unit (AAU) [27]. This transition from a two-level structure in 4G to a three-level design (CU + DU + AAU) in 5G networks represents the next step in wireless network evolution. According to [28], this functional separation assigns the DU to manage the physical, MAC, and radio link control (RLC) sublayers, while the CU oversees the packet data convergence protocol (PDCP), service data adaptation protocol (SDAP), and radio resource control (RRC) sublayers. Additionally, the 5G mobile system's access network incorporates enabling technologies such as millimeter wave (mmW), massive MIMO (mMIMO), heterogeneous networks (HetNets), and ultra-dense networks [4]. According to [29], mmW technologies enhance transmission rates by expanding the available bandwidth, increasing transmission frequencies from 30 GHz to 300 GHz. However, mmW technologies are limited to small cells due to a significant attenuation at high frequencies [30]. mMIMO improves spectrum utilization and data transmission rates by connecting multiple antennas to a single BS [31]. Effective beamforming and spatial multiplexing, key properties of mMIMO, also help reduce interference. Nonetheless, challenges such as pilot contamination and channel correlation must be addressed to fully realize mMIMO's potential.

It is to be noted that mMIMO technology can be implemented across different frequency bands, including millimeter waves (mmWave) to improve the multiplexing capabilities of a large number of antennae. The specific frequency bands and the power requirement of the transmission medium were not considered when elaborating the power consumption models in this study

The power consumption model for the mMIMO BSs used in this study is adapted from [4] and is formulated as follows:

$$PW_{BS} = \frac{K \cdot PW_{UE}}{\eta PA} + PW_{CP}^{li} + X_3 K^3 + Y_0 N + Y_1 N \cdot K + Y_2 N \cdot K^2 + AK \cdot R_{UE} \tag{1}$$

In Equation (1), K is the quantity of user equipment (UEs) that are in active mode, PW_{UE} is the UE output power (downlink), ηPA is the power amplifier efficiency, N is the quantity of antennae deployed at the BS, X_3 is the beamforming processing component that has a linear variation with K^3, Y_0 is the power consumed by each transceiver module that is connected to all of the antennae, Y_1 is the beamforming processing component that has a linear variation with $N.K$, Y_2 is the aggregation of the contributions of the beamforming processing and channel estimation and that has a linear variation with $N.K^2$, R_{UE} is the throughput of UE, A is the aggregation of the power consumption needed by the coding/decoding operations and is a part of a backhaul network that is independent of load, per bit of information, and PW_{CP}^{li} is the power consumed in the circuit, independent of load.

3.1.2. Backhaul Power Consumption (PW_{BL})

Fiber backhaul is extensively recognized as the preferred option for 5G deployment among mobile network operators. Furthermore, as previously mentioned, GPON and NGPON are anticipated to be the most widely implemented access networks globally over the next four years [32]. Consequently, this work considers GPON/NGPON as the backhaul network technology for various 5G deployment scenarios, as depicted in Figure 2. In this setup, the RU is connected to an ONT, collocated on the cell site. The ONT is connected to the optical line terminal, usually located in a central office through the optical distribution network. The OLT connects to the core network via the gateway equipment.
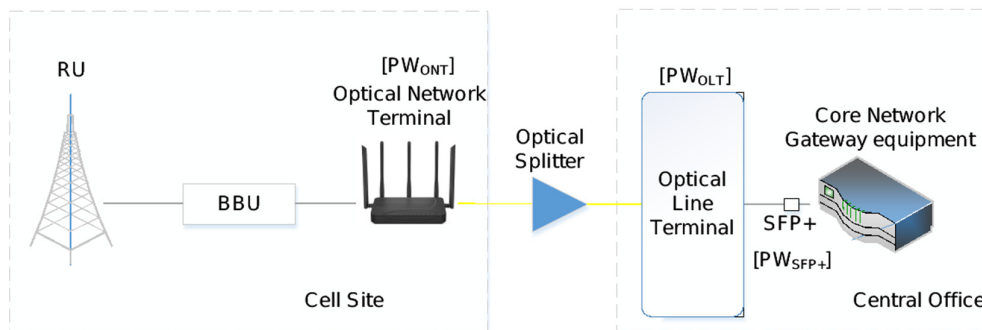

Figure 2. Backhaul connectivity over GPON/NGPON technology.

According to [18,33,34], the overall energy consumption is the sum of the energy used by all of the active devices and systems within the network architecture under consideration. Consequently, the power consumption of the backhaul network, denoted as PW_{BL}, for the GPON/NGPON scenario is calculated as follows:

$$PW_{BL} = N_{BS}PW_{ONT} + N_{OLT}PW_{OLT} + N_{SFP+}PW_{SFP+} \tag{2}$$

In Equation (2), N_{BS} is the number of BSs in the network, PW_{ONT} is the power consumed by an ONT, N_{OLT} is the ratio $[\frac{N_{ONT}}{N_{Splitter\ Ports}\ N_{OLT\ Cards}}]$, N_{ONT} is the total number of $ONTs$ being used in the network, $N_{Splitter\ Ports}$ is the total quantity of splitter ports utilized to establish the necessary connections for $ONTs$, $N_{OLT\ Cards}$ is the total number of OLT cards, N_{SFP+} pertains to the total number of $SFPs$ (small form-factor pluggable modules) installed within the network, and PW_{SFP+} is the power consumed by each of the SFPs. Alternatively, the power consumption of the backhaul network, denoted as PW_{BL}, for a point-to-point scenario is determined as follows:

$$PW_{BL} = N_{BS}PW_{GES} + N_{SFP+}PW_{SFP+} \tag{3}$$

where PW_{GES} is the power consumption of the Giga Ethernet (GE) switch at the cell site, N_{SFP+} represents the total quantity of *SFPs* installed within the network, and PW_{SFP+} represents the power consumption of each of the *SFPs*.

3.1.3. Power Usage at the Core Network Level

Software-Defined Networking (SDN), recognized as a crucial technology for orchestrating and managing applications and services in 5G networks to enhance efficiency [35], has been adopted at the Core Network level in this study across various network architectures. SDN has been considered as it is the main core network component of 5G. Figure 3 presents a simplified SDN architecture to elaborate on the power consumptions models derived in this paper. The main purpose of implementing SDN technology is to simplify the configuration of the core network and to increase the flexibility to adapt to traffic requirements. The control plane has the responsibility of managing and controlling the network whilst the data plane, comprising the connected switches, regulates the forwarding of packets based on rules according to the flow tables loaded on the switches by the controller.

In this study, the power model for the 5G core network is adapted from the works of [13,24]. The power consumption of the SDN-based core network, denoted as PW_{SDN}, consists of three main components: controllers, switches, and Ethernet links. This model is further corroborated by [12], which illustrates how SDN centralizes control plane functions from forwarding devices, such as switches and routers, onto an SDN controller.
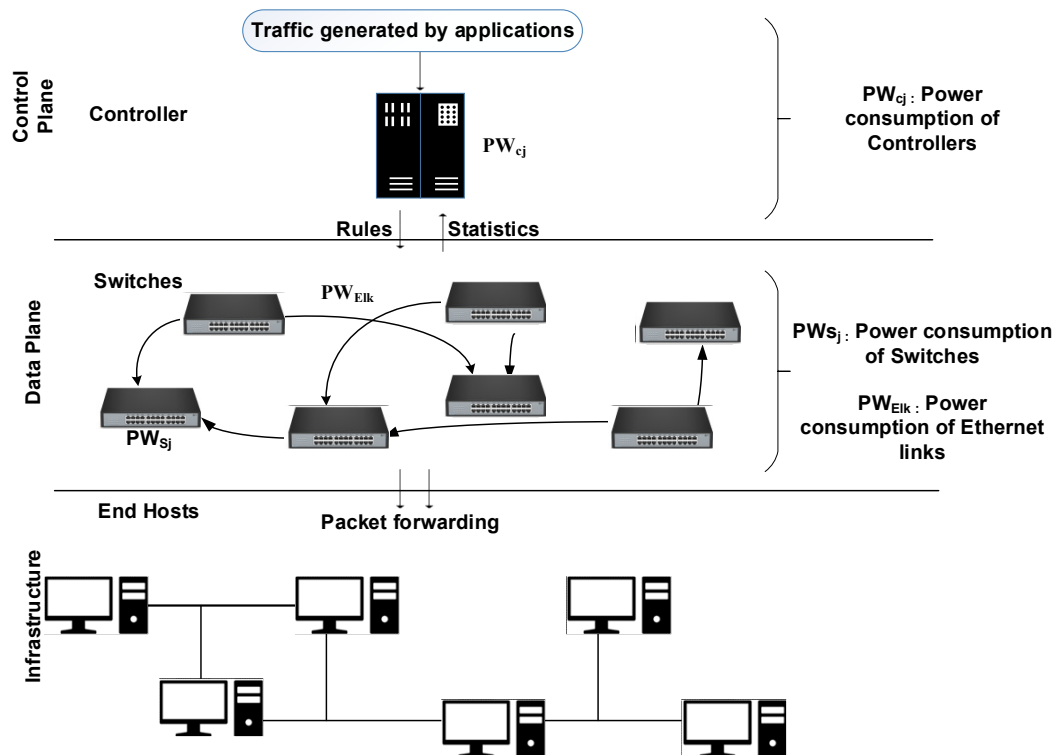

Figure 3. SDN architecture (adapted from [12]).

In this study, the power model for the 5G core network is adapted from the works of [13,24]. The power consumption of the SDN-based core network, denoted as PW_{SDN}, consists of three main components: controllers, switches, and Ethernet links. This model is further corroborated by [36], which illustrates how SDN centralizes control plane

functions from forwarding devices, such as switches and routers, onto an SDN controller. Consequently, in this research, the power consumption at the core network level, PW_{SDN}, is considered to be the sum of the power usage of the various elements that make up the SDN architecture, which is outlined below, as follows:

$$PW_{SDN} = \sum_{j=1}^{n}(z_{1j} \times PW_{Sj} + z_{2j} \times PW_{cj} + z_{3j} \times L) + PW_{Elk} \tag{4}$$

where PW_{cj} is the power consumption of the controllers, PW_{sj} is the power consumption of the switches, PW_{Elk} is the power consumed by the ethernet links, n represents the total number of network elements, including switches, controllers, and latency queues, L represents the packets queued due to latency, and z_1, z_2, and z_3 are the constants derived from the simulation based on the policy decisions of the SDN controller.

3.1.4. End-to-End Power Consumption (PW$_{DEC}$)

Using Equations (1), (2), and (4), the end-to-end power consumption, denoted as PW_{Dec}, for a 5G D-RAN incorporating mMIMO technology, can be calculated as follows:

$$
\begin{aligned}
PW_{Dec} &= PW_{BS} + PW_{BL} + PW_{SDN} \\
&= \sum_{i=1}^{T}\left(\frac{K \cdot PW_{UE}}{\eta PA} + PW_{CP}^{li} + X_3 K^3 + Y_0 N + Y_1 N \cdot K + Y_2 N \cdot K^2 + AK \cdot R_{UE}\right) + \\
&\quad N_{BS} PW_{ONT} + \qquad\qquad N_{OLT} PW_{OLT} + N_{SFP+} PW_{SFP+} + \sum_{j=1}^{n}(z_{1j} \times PW_{Si} + \\
&\quad z_{2j} \times PW_{cj} + z_{3j} \times L) + PW_{Elk}
\end{aligned}
\tag{5}
$$

where T is the total number of BSs in the network, PW_{SDN} is the power consumed by the SDN-based Core Network, and PW_{BL} is the backhaul network energy consumption. The remaining parameters are specified in Equations (1), (2), and (4). Passive Optical Networks (PONs) are recognized as a reliable, resilient, and cost-effective solution for 5G backhaul connectivity, as elaborated in [37,38]. Consequently, this 5G network model assumes a GPON/NGPON backhaul integrated with a fully SDN-based core network.

3.2. End-to-End Power Consumption Model for Centralized RAN Architecture

In a centralized configuration, such as the 5G-Cloud D-RAN, the DU and RU operations are conducted on-site. Conversely, the CU functionalities are performed remotely on specialized hardware. This is in contrast to a decentralized configuration. In Figure 4, the NG-RAN design, which includes the RUs linked to the DUs through the front-haul interface, is illustrated. The mid-haul links allow for the connection of numerous DUs to a single CU. Conversely, the backhaul cables connect the CUs to the 5G core network as shown in Figure 4. On the RAN side, several DUs, interconnected via the fronthaul links, may be bound to a particular CU. It is to be noted that the functions of the CUs and the DUs can be implemented either on dedicated bare metal servers or in virtual environments in a cloud network. Thus, the RAN power consumption is the aggregation of the power consumed by the BSs, including the CUs and mid-haul links.
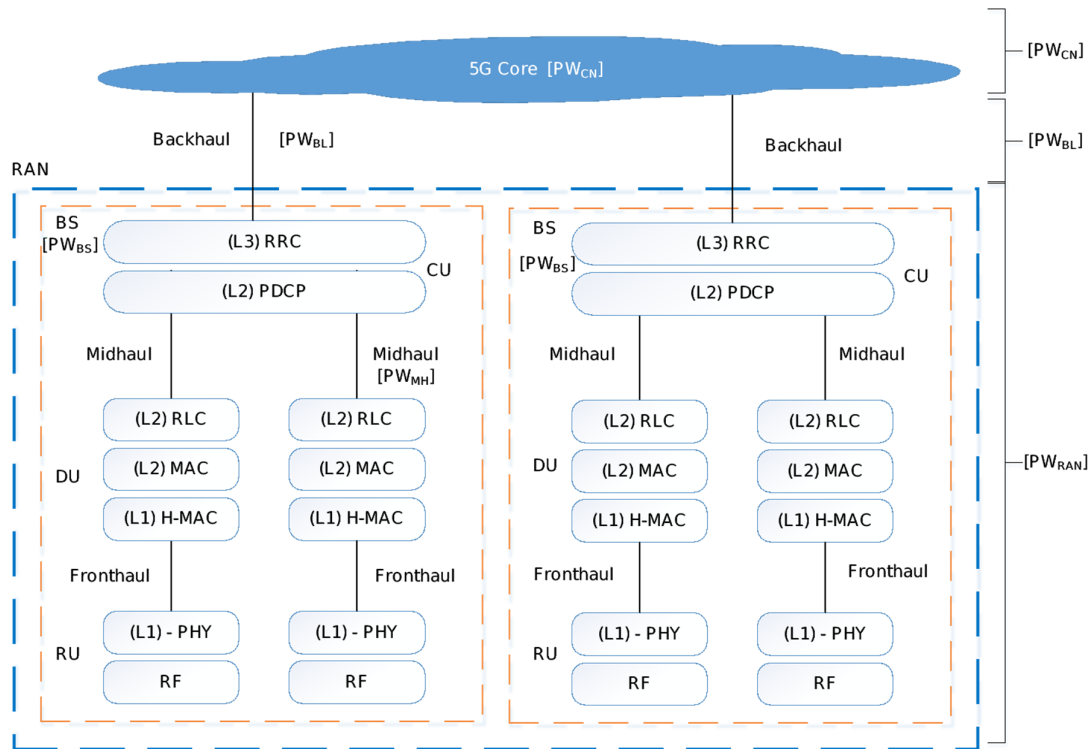
Figure 4. NG-RAN architecture (adapted from [4]).

In line with previous works carried out by [4,34], the power consumed by the *i-th* BS in the C-RAN architecture, PW_{BS_i}, in this research is formulated as follows:

$$\sum_i PW_{BS_i} = \sum_i PW_{DU_i} \left(1 - \frac{PW_{CO_i} + PW_{NF_i}}{100}\right) + PW_{CU} \tag{6}$$

where PW_{DU_i} refers to the power consumed by the i-th implemented DU, PW_{CU} is the power usage of the BBU host where the CU is situated, PW_{NF_i} is the network functions' proportion of the power usage shifted to the CU, and PW_{CO_i} is the proportion of the cooling power usage related to the *i-th* DU. The power used by the BBU host can be derived as follows:

$$PW_{CU} = \sum_i PW_{DU_i} \left(\frac{1/Ga_{CO}}{100} + \frac{PW_{NF_i}/N_{BS}}{100}\left[\frac{N_{BS}}{Ga_{st}\,Ga_{po}}\right]PW_{add}\right) \tag{7}$$

where Ga_{CO} represents the cooling gain, Ga_{st} denotes the stacking gain, Ga_{pot} refers to the pooling gain, and PW_{add} represents the additional power usage in BBU due to resource pooling. It should be emphasized that Equation (7) is based on the assumption that the CU is deployed in a dedicated bare metal environment, similar to that utilized for a single DU.

Power utilized by the DU, PW_{DU}, may be calculated using Equation (1), which additionally accounts for the power consumption by the RU and front link. Therefore, a generalized equation for the overall power used by the RAN can be evaluated as follows:

$$PW_{RAN} = \sum_i PW_{BS_i} + \sum_i PW_{MH_i} + \sum_k PW_{CU_K} \tag{8}$$

where PW_{BS_i} is the power used by the *i-th* BS (gNB), PW_{MH_i} is the power used by the i-th mid-haul link, and PW_{CU_i} is the power used by the i-th CU. The power consumed by the mid-haul segment varies according to the transport network technology selected, the total number of BSs installed in the RAN, and the capacity requirement for each BS. Ref. [4] assumed a scenario that involved optical dense wavelength division multiplexing

technology to form a ring architecture. In this case, the power usage in the mid-haul segment is derived as follows:

$$PW_{MH_i} = \left\lceil \frac{BW_{S_i}}{R_{tx}} \right\rceil \left(2 \cdot PW_{tx} + \frac{PW_{xc}}{N_f} \right) \tag{9}$$

where BW_{S_i} is the capacity of the transport network required at the i-th BS considering the functional split, R_{tx} is the rate of the transport network in Gbps, PW_{tx} is the transport network node's power usage, PW_{xc} is the power consumed by the ports that cross connect on the transport network, and N_f constitutes the number of wavelengths per fibre. So, for a 5G CRAN network implemented on a hardware infrastructure, the end-to-end power consumption, PW_{HCR}, is stated as follows:

$$PW_{HCR} = PW_{RAN} + PW_{BL} + PW_{CN} \tag{10}$$

By rewriting Equation (10), the following power usage model is obtained as follows:

$$PW_{HCR} = \sum_i PW_{DU_i} \left(1 - \frac{PW_{CO_j} + PW_{NF_j}}{100} \right) + \sum_i PW_{DU_i} \left(\frac{1/Ga_{CO}}{100} + \right.$$

$$\frac{PW_{NF_j}/N_{BS}}{100} \left[\frac{N_{BS}}{Ga_{st} \, Ga_{po}} \right] PW_{add} \Bigg) +$$

$$\left\lceil \frac{BW_{S_i}}{R_{tx}} \right\rceil \left(2 \cdot PW_{tx} + \frac{PW_{xc}}{N_f} \right) + N_{BS} PW_{GES} + N_{SFP} PW_{SFP} +$$

$$\sum_{j=1}^{n} (z_{1j} \times PW_{Sj} + z_{2j} \times PW_{cj} + z_{3j} \times L) + PW_{Elk} \tag{11}$$

Equation (11) uses the same parameters as Equations (3)–(9). It can be anticipated that GPON/NGPON technology will be used to deploy the backhaul segment, with the core network configured with full SDN capability.

3.3. End-to-End Power Consumption for 5G Cloud C-RAN

The end-to-end power consumption model developed in this study for a 5G Cloud C-RAN network in which the RAN is virtualized is based on [10,39]. The model is based on three layers, namely the central cloud site (CCS), the remote sites (RMS), and the cell layer site (CLS). The CCS is responsible for a portion of the processing needed at the RMS. The latter manages the RUs deployed in the CLS for interconnecting the user devices to the network. The power consumed by the front-haul and mid-haul segments serves as the basis for calculating the total power consumption for the 5G virtualized RAN scenario. The front-haul power consumption is calculated using the power consumed by the RRU and the RMS links. Figure 5 depicts the mid-haul consumption, which includes both the central cloud site and the remote site.
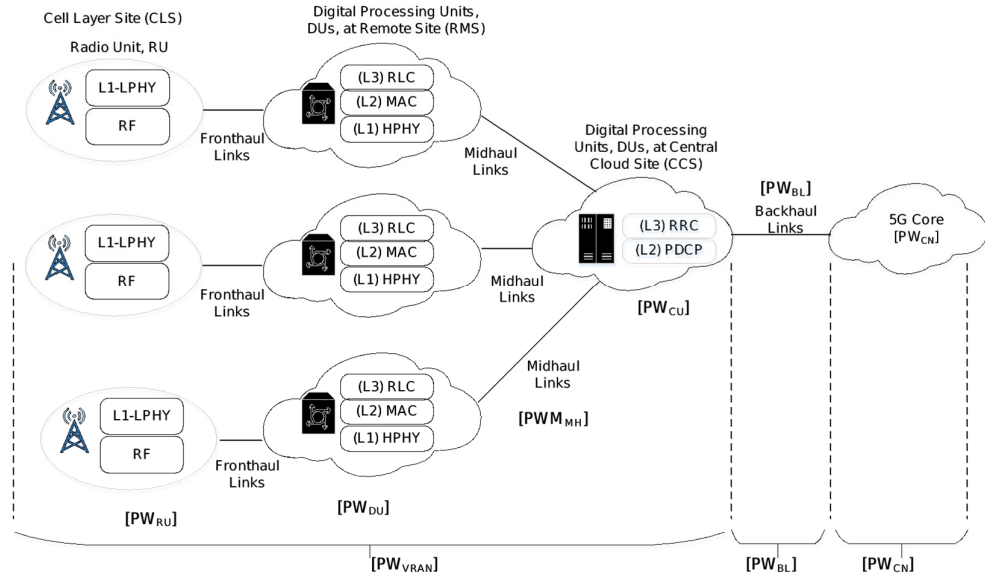
Figure 5. A standard Cloud C-RAN power consumption model with virtualized CU and DU.

The power used by a virtualized RAN, PW$_{VRAN}$, can be derived as follows:

$$PW_{VRAN} = N_{RU} \ (PW_{RU} + PW_{Lk}) + F_{CS}PW_{CU} + (1 - F_{CS})PW_{DU} \qquad (12)$$

where N_{RU} is the sum of RUs in the network, PW_{RU} is the power attributed to an RU, PW_{Lk} is the links' power consumption, F_{CS} is the function split from the cloud site, PW_{DU} is the power used by the DU (remote site), and PW_{CU} is the power used by the CU (central site). The RU's power consumption model is based on [10]. This study presents the RU's power consumption as a function of its operating mode. PW$_S$ stands for power used when there aren't many active users in sleep mode, and PW$_A$ stands for power used when there are active users. Thus, the following formula is used to determine the power used by the RUs, PW$_{RU}$, as follows:

$$PW_{RU} = YPW_A + (1 - y)PW_S \qquad (13)$$

where PW_A represents the active mode power consumption of the *RUs*, Y is the proportion of active *RUs* expressed as a percentage, PW_S is the sleep mode power consumption of the *RUs*. PW_A can be derived as follows:

$$PW_A = PW_{fx} + Y_{UD} \frac{PW_{am}^{max}}{\propto} \qquad (14)$$

where PW_{fx} is the constant power usage in each RU, Y_{UD} is the mean quantity of user devices (UDs) connected to each RU, PW_{am}^{max} is the upper threshold for the power amplifier's power, and $\propto$ is the factor for direct current to radio frequency conversion. Presumably, PW_{Lk} is estimated similarly as PW_{MH_i} for the C-RAN scenario. Also, since it represents the power consumption of mid-haul links between the remote sites and central sites, the end-to-end power usage for a 5G Cloud C-RAN, PW$_{VCR}$, can be evaluated as follows:

$$PW_{VCR} = PW_{VRAN} + PW_{BL} + PW_{CN} \qquad (15)$$

By rewriting Equation (15), the following power usage model is derived as follows:

$$PW_{VCR} = N_{RU} \left[\left(Y[PW_{fx} + Y_{UD} \, PW_{am}^{max}/\propto] \quad + (1-y)PW_S + \right. \right.$$

$$\left. \left[\frac{BW}{R_{tx}} \right] \left(2 \cdot PW_{tx} + \frac{PW_{xc}}{N_f} \right) \right] + \qquad F_{CS}PW_{CU} + (1 -$$

$$F_{CS})PW_{DU} + N_{BS}PW_{GES} + N_{SFP}PW_{SFP} + \qquad (16)$$

$$\sum_{j=1}^{n} (z_{1j} * PW_{Sj} + z_{2j} * PW_{cj} + z_{3j} * L) + PW_{Elk}$$

Equations (4), (7)–(10), and (12)–(14) describe the parameters used in Equation (16). Further, for the reasons mentioned previously, it is presumed that the backhaul employs GPON/NGPON technology, while a complete SDN is implemented at the core network level.

4. Findings and Discussion

Based on the power ratings of the various components used in 5G RAN and the typical values provided in the literature, this Section projects some real power consumption figures using the three power models that were developed in Section 3 under typical scenarios.

4.1. Power Usage of 5G D-RAN

Equation (1) provided the power consumption model of the mMIMO BS deployed in the 5G D-RAN scenario, as suggested by [4,40] and detailed in Section 3.1. Table 1 provides a summary of some of the typical values of the parameters given in Equation (1) in the works under discussion.

Table 1. Typical parametric settings for the 5G D-RAN scenario's mMIMO power consumption model.

Parameter	Value
ηPA	0.39
X_3	10^{-7} [W]
Y_1	3×10^{-3} [W]
A	1.15 [W/Gbps]
PW_{CP}^{li}	20 [W]
Y_0	1 [W]
Y_2	9.4×10^{-7} [W]

Ref. [9] examined the effects of mMIMO on the ratio of users to active antennas attached to a BS under three different network loads. The active antennae unit and user counts were used to create the models for BS power consumption. According to [4], a system's optimal energy efficiency is defined by a nearly linear relationship between the number of active antennae (K) and user devices (N). Each antenna was assumed to have a 0.1 W transmission power. Furthermore, Ref. [41] has demonstrated that the transmit power varied roughly linearly with the number of installed antennae for the mMIMO systems' energy efficiency optimization. A mMIMO-based BS implemented in the 5G D-RAN topology is examined for the following scenarios in order to extrapolate the results from [9,41]: In Equation (1), K is changed while all of the other values remain constant, and N is changed while all of the other parameters remain constant.

Using the normal values from [4] and assuming a constant number of 50 active users with a throughput of 1 Gbps, Equation (1) yielded the following results for the base station power consumption, as illustrated in Figure 6.
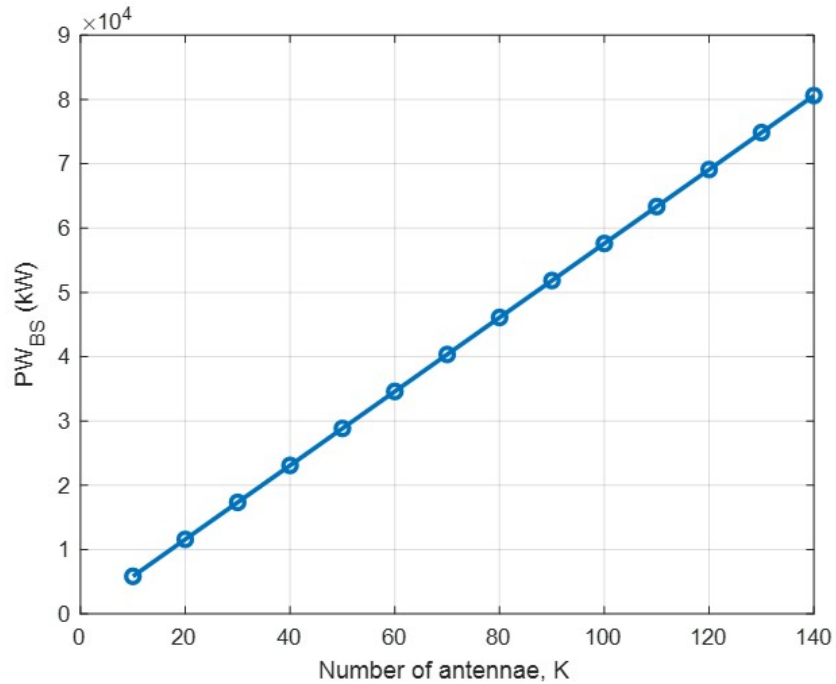
Figure 6. A variation of the BS power consumption (PW_{BS}) with K.

Figure 6 shows that the PW$_{BS}$ rises approximately linearly as the number of antennae increases. When 140 antennae are installed, the consumption peaks at 80 kW, with an average increase of about 600 kW for each new antenna. The results for the PW_{BS} change with respect to N are likewise shown in Figure 7. Notably, 115 active antennae were deemed sufficient based on the presumptions and standard values in [9,41]. A maximum cell radius of 500 m and the uniform distribution of users within a radius of 35 m from the cell core are two crucial model assumptions.
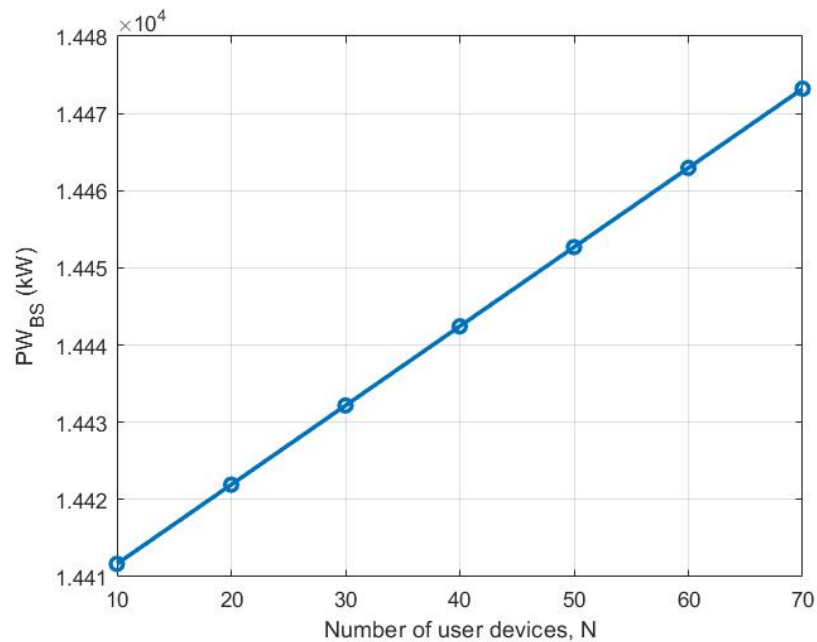

Figure 7. Variation of the PW_{BS} with N.

With a high consumption of 14,453 kW recorded for 50 users, Figure 7 shows that the PW$_{BS}$ rises linearly with the number of active users. Conversely, Equation (2) provides the power consumption of the GPON/NGPON-based backhaul, or PWBL. Table 2 lists the backhaul network's typical power usage as provided in [15,11].

Table 2. Typical power consumption values for the GPON/NGPON backhaul.

Equipment/Component	Typical Power Usage
Optical Line Terminal (OLT)—Backhaul	105 W
Optical Network Terminal (ONT)—Backhaul	24 W
SFP+	4 W
Core Router	500 W

It can be assumed that each RU in the 5G network has an optical network terminal (ONT) that links to a single optical line terminal (OLT) in order to assess the power consumption of the GPON/NGPON backhaul. The fact that PON is a point-to-multipoint technology with a physical range of up to 60 km lends credence to this [38]. Equation (2) can be modified as follows to determine the backhaul power usage, utilizing the configuration shown in Figure 2:

$$PW_{BL} = N_{RU}PW_{ONT} + N_{OLT}PW_{OLT} + (2 + N_{RU}) \times PW_{SFP+}PW_{NG} \quad (17)$$

where N_{RU} is the number of *RUs*, PW_{NG} is the network gateway switch's power usage, and the remaining parameters are described in Equation (2). Since heterogeneous and ultra-dense networks are key technical enablers for 5G, it is imperative to investigate how RU deployment impacts the end-to-end power consumption of 5G networks [35]. Figure 8 illustrates how the backhaul's power usage varies with the number of *RUs*, as noted in [15]. It shows that the power loss coefficient (*PW$_{BL}$*) grows almost linearly with the 5G network's RU count, rising by around 20 W per RU on average.
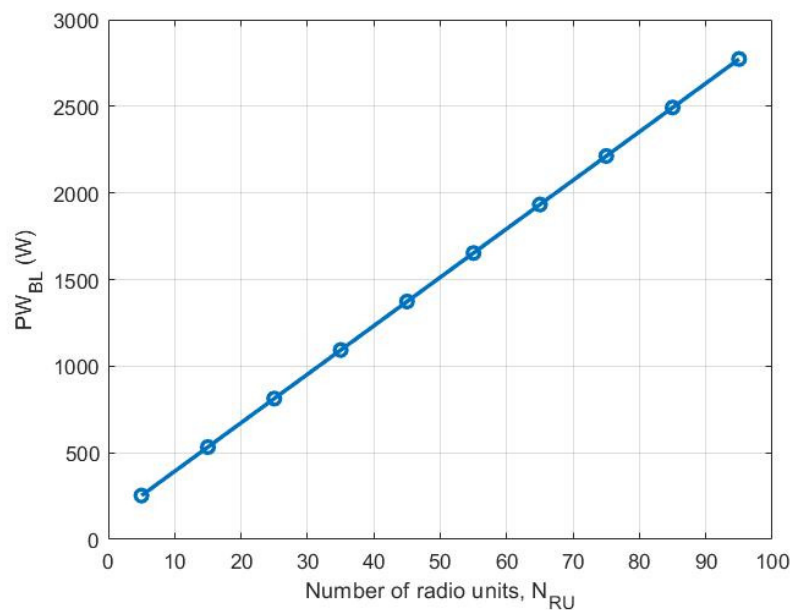

Figure 8. Variation of the PW_{BL} with the number of RUs.

Equation (4) in Section 3.1.3 provides the core network's power consumption model. Table 3 presents the typical values that were provided in [11,13] for the computation of SDN-based core networks for various network sizes.

Table 3. Common parametric settings for power consumption in the core network.

Parameter	Typical Value
PW_{Si}	1 kW
PW_{cj}	2 kW
z_{1j}	0.5
z_{2j}	0.75
z_{3j}	0.8
L	6
PW_{Elk}	0.5 W (Per link)

According to [42], in order to attain the best possible balance between dependability and latency, it is also assumed that each controller switch is connected to four open flow switches on average. Figure 9 illustrates the anticipated correlation between a network's size, n, and the power consumption of its core network based on the data utilized in [13].
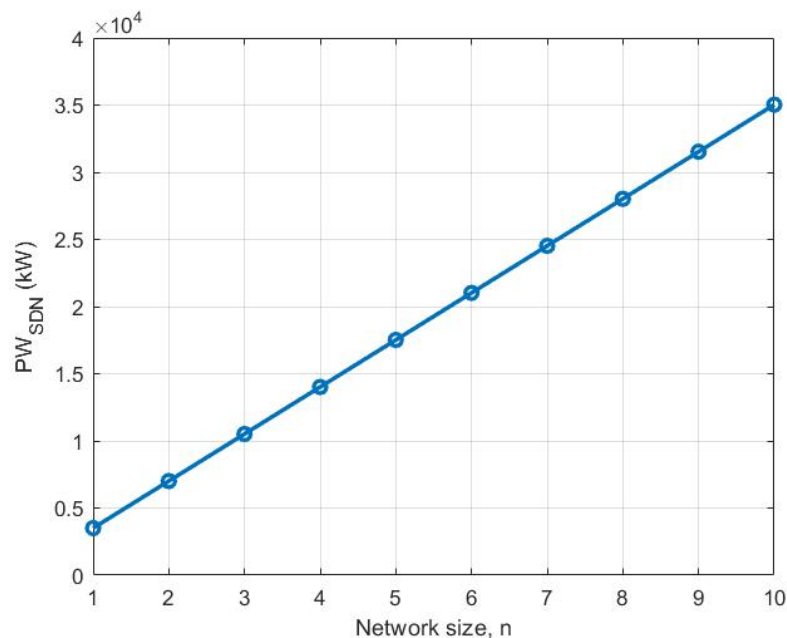

Figure 9. A variation of the core network power consumption with network size (*n*).

It is evident that the power consumption of the core network increases linearly with network size, with each node consuming an average of roughly 3300 kW of power. By guaranteeing a uniform flow of traffic across the different nodes, the SDN controller's function in controlling data flow elements and establishing connections throughout the whole network explains the linear relationship [42]. The various components of a 5G D-RAN network architecture are made up of the power consumption at the base station, backhaul links, and the core network, which are combined as stated in Equation (5) in Section 3.2. To assess the end-to-end power consumption of a 5G D-RAN, the following assumptions are made as follows: According to the deployment density proposed in [4], the number of active antennae is regarded as the primary dependent variable since BSs are responsible for up to 80% of the total power consumption. The simulations conducted in [4] show that an average value of 50 is assumed for N_{RU}. At the core network level, the end-to-end power consumption is assessed under a 100% network load maximum, and an average value of N = 50 is considered for the number of active users in a mMIMO BS scenario. These presumptions are meant to guarantee that the best possible balance

between dependability and latency is achieved by optimizing each data flow piece and the link that goes with it.

The end-to-end network power consumption is shown in Figure 10 after considering all the factors mentioned above.
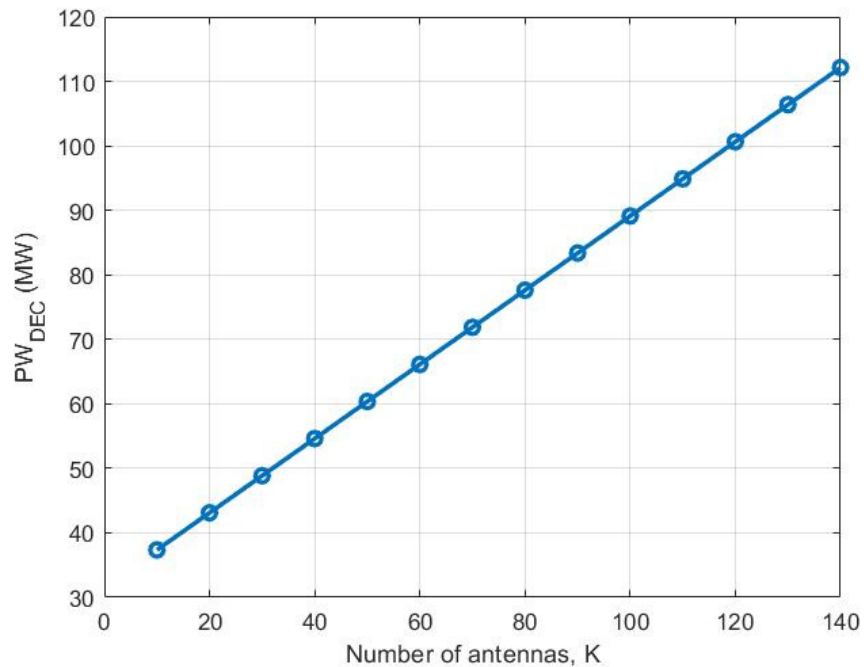

Figure 10. Changes in the end-to-end power usage for 5G D-RAN scenarios based on the number of active antennae.

After taking into account all of the previously discussed criteria, Figure 11 shows the end-to-end network power usage. From Figure 11, it is evident that the power consumption rises in a nearly linear fashion as the number of active antennae increases. As K changes from 30 to 120, the power consumption per antenna increases by about 0.6 MW. When 140 antennae are deployed, the 5G D-RAN's power usage reaches a peak of 112 MW. Additionally, the breakdown of the total power consumption at the various 5G D-RAN segments with an average of 115 active antennae is depicted in the bar chart in Figure 11.

Figure 11 illustrates that the BS is responsible for approximately 68%, or 65 MW, of the 5G D-RAN model's total power usage of 95 MW. These results support previous studies that found that in 5G mobile networks, BSs can use up to 80% of the power [35]. The findings in Figure 11 contribute to the body of literature by exposing the end-to-end power consumption of the 5G D-RAN and providing a more comprehensive examination of power consumption.

Figure 11. Breakdown of the 5G-DRAN's end-to-end power usage.

Figure 11 illustrates that the BS is responsible for approximately 68%, or 65 MW, of the 5G D-RAN model's total power usage of 95 MW. These results support previous studies that found that in 5G mobile networks, BSs can use up to 80% of the power [35]. The findings in Figure 11 contribute to the body of literature by exposing the end-to-end power consumption of the 5G D-RAN and providing a more comprehensive examination of power consumption.
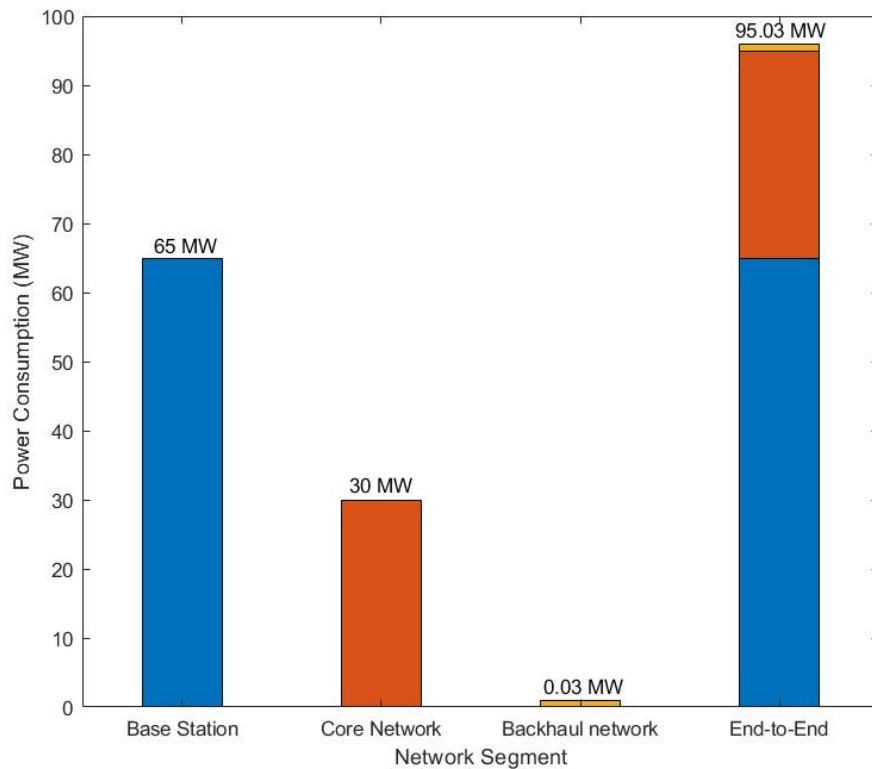
4.2. Power Usage of 5G C-RAN

As previously said, Equation (6) in Section 3.2 can be used to compute the power consumption for the i-th BS in a C-RAN, PW_{BSi}. Table 4 reports some of the typical values of the parameters given in Equation (7), which were suggested in [4].

Table 4. Common parametric settings for the Base Station power consumption for the Centralized RAN.

Parameter	Typical Value
PW_{CO}	10
PW_{NF}	15
GA_{CO}	0.2
GA_{ST}	2
N_{BS}	10
Ga_{po}	5
PW_{add}	2 W

Figure 12 illustrates how the PW_{BS} varies with K for the 5G C-RAN scenario, based on the typical values of the parameters listed in Tables 2–4.
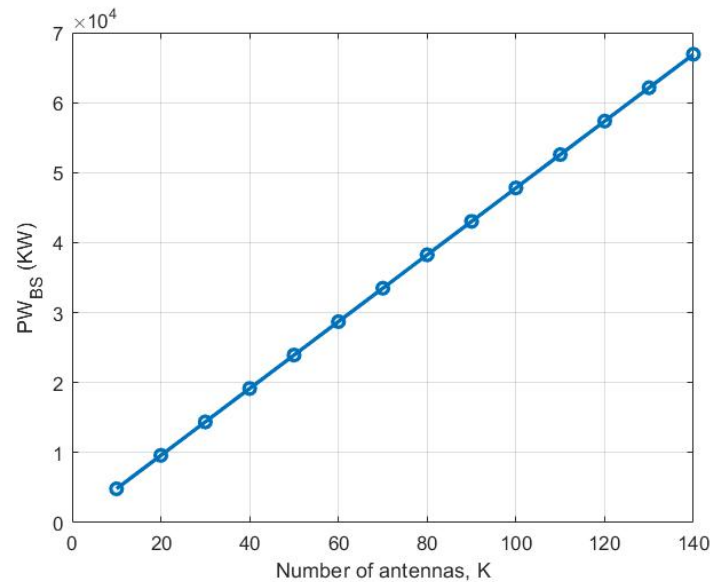

Figure 12. Changes in the 5G C-RAN scenario's BS power consumption with active antennas.

The mid-haul power consumption, PW_{MH}, was calculated using a ring architecture based on optical dense wavelength multiplexing, as described in Equation (9) (see Section 3.2). According to Equation (9), the mid-haul power consumption is dependent on the number of wavelengths per fiber, the rate, and the power used by the transport network nodes. According to the data presented in [43], this analysis used typical rates of transport network nodes based on the type of SFP being deployed. Figure 13 illustrates the relationship between the variation of mid-haul power consumption per port and the corresponding transmission rate, which is obtained by modifying the standard parameter values from [4] to the architectures taken into consideration in this work. It is evident that with higher transmission speeds of the order of 100 Gbps, the mid-haul power usage drops below 10 W. This is because technology like wavelength division multiplexing require fewer ports.
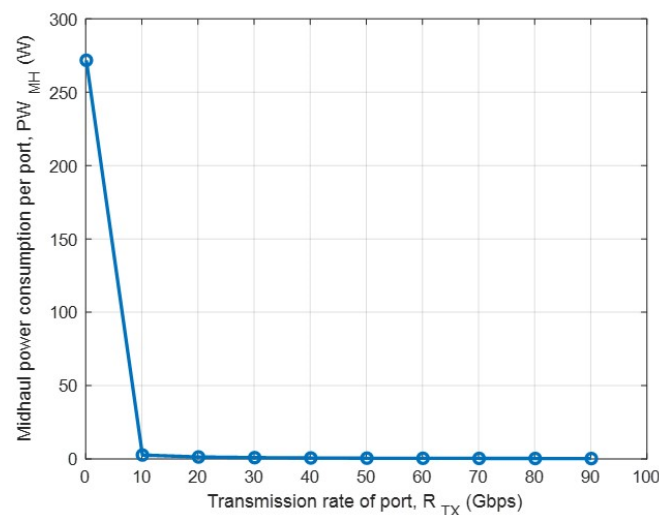

Figure 13. Power usage per port during the mid-haul changes with transmission rate.

The end-to-end power consumption, PW$_{HCR}$, for a 5G network implemented with hardware-based C-RAN is described in Section 3.3, Equation (11). The majority of the power consumption in the 5G D-RAN design is found to occur at the BS level. Therefore, K, the dependent variable, and the values from Tables 1 and 2 have been used to determine the end-to-end power consumption for the 5G D-RAN scenario. According to prior relevant works conducted [43], it is believed that 31-Gbps ports are used for mid-haul connectivity. The link between a 5G C-RAN's overall power usage and the number of active antennae, K, is shown in Figure 14.
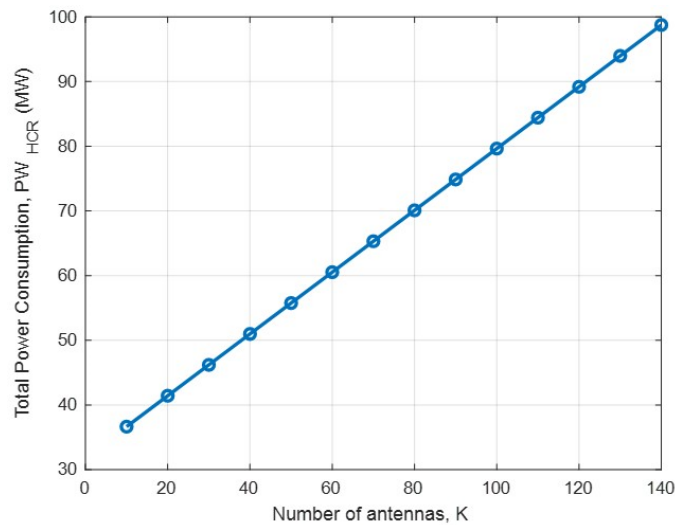

Figure 14. The change in the total power consumption of 5G C-RAN with K.

The overall power usage trend is rather comparable to that of the 5G D-RAN scenario, as shown in Figure 14. However, for the corresponding K, the centralized 5G scenario's end-to-end power usage (84 MW) is around 12% lower than the decentralized topology's (95 MW). The breakdown of the total power consumption at the various network segments of the 5G C-RAN is further depicted by the bar chart in Figure 15.
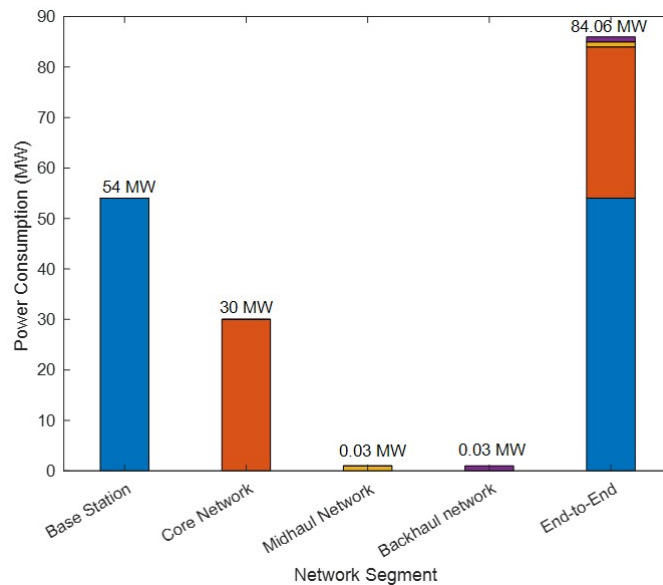

Figure 15. Power consumption breakdown for the various network segments in a 5G C-RAN scenario.

According to Figure 15, the BS uses about 54 MW of power, or about 65% of the network's total consumption of 84 MW. This result is in line with past studies [5,35], that have demonstrated that in a 5G centralized network, the base station (BS) can be responsible for up to 75% of the overall power consumption. Figure 15 further demonstrates that the 5G C-RAN model uses about 12% less energy (84 MW) than the prior estimate (95 MW) for the 5G D-RAN scenario. The findings are consistent with earlier studies that demonstrate how dynamic computational resource allocation in centralized 5G networks can lower the power consumption [44,45].

4.3. Power Usage of 5G Cloud C-RAN

According to [45], Equation (12), which is described in Section 3.3, can be used to calculate the overall power consumption, or PW$_{\text{VRAN}}$, in a 5G Cloud C-RAN scenario. For 5G Cloud C-RAN architectures implemented with virtualized CUs and DUs, the end-to-end power consumption, PW$_{\text{VCR}}$, is defined by Equation (16) in Section 3.3. The parametric parameters for the virtualized RAN power consumption, which were taken from the work of [10], are shown in Table 5.

Table 5. Typical parametric settings for the virtualized RAN power consumption.

Parameter	Typical Value
N_{RU}	100
Y	0.4, 0.6, 0.8, 1.0
PW_{fx}	2 W
Y_{UD}	15
PW_{am}^{max}	0.13
$\propto$	1
PW_S	1
F_{CS}	0-1
PW_{CU}	100
PW_{DU}	20

Tables 1 and 2 previously described the parametric values for the network's core, mid-haul, and backhaul power consumption. The ratio of active remote RUs (*Y*) is the main parameter taken into account when evaluating power consumption in the virtualized RAN (VRAN). This is because, in relation to the total number of users, *Y* represents the percentage of RRUs that are actively contributing. RRUs are the main energy consumers in the virtualized RAN, as was previously mentioned. The link between the ratio of active RRUs (*Y*) and the power consumption (PW$_{\text{VCR}}$) of the virtualized RAN is shown in Figure 16.

Figure 16 illustrates how PW$_{\text{VRAN}}$ rises nearly linearly as the proportion of active RRUs rises. A 10% increase in Y results in an equivalent PWVRAN increase of about 3 MW. PW$_{\text{VRAN}}$ reaches a peak value of 47 MW while all of the RRUs are operating. Following an analysis of the VRAN 5G network scenario, it was discovered that the BS was mostly to blame for the power usage. Therefore, using the information in Tables 1, 2, and 3, the end-to-end power consumption of the 5G VRAN architecture (PW$_{\text{VRAN}}$) has been calculated, with the ratio of active RUs, Y, serving as the dependent variable. Additionally, it is estimated that each RU has an average of fifteen user devices [10]. This assumption is justified by the fact that a minimum number of active RRUs and DUs for such a high number of user devices is required to ensure the greatest possible balance between network efficiency and dependability.

Figure 16. VRAN power usage fluctuation with active RRUs.

Additionally, it is estimated that each RU has an average of fifteen user devices [10]. This assumption is justified by the fact that a minimum number of active RRUs and DUs for such a high number of user devices is required to ensure the greatest possible 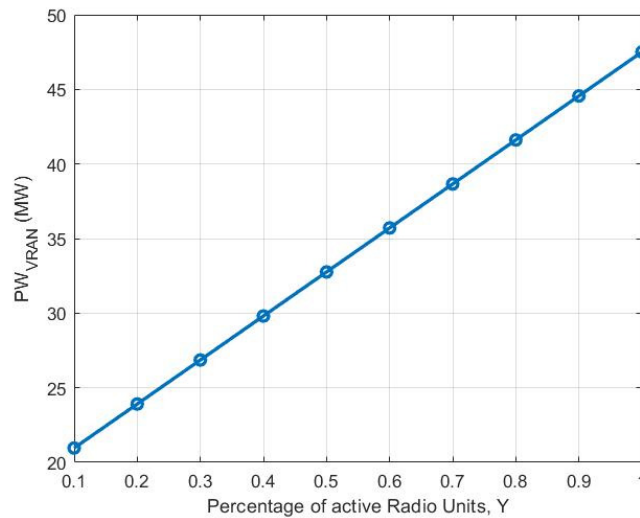balance between network efficiency and dependability. The power consumption variation of a 5G network based on VRAN in relation to Y is shown in Figure 17.
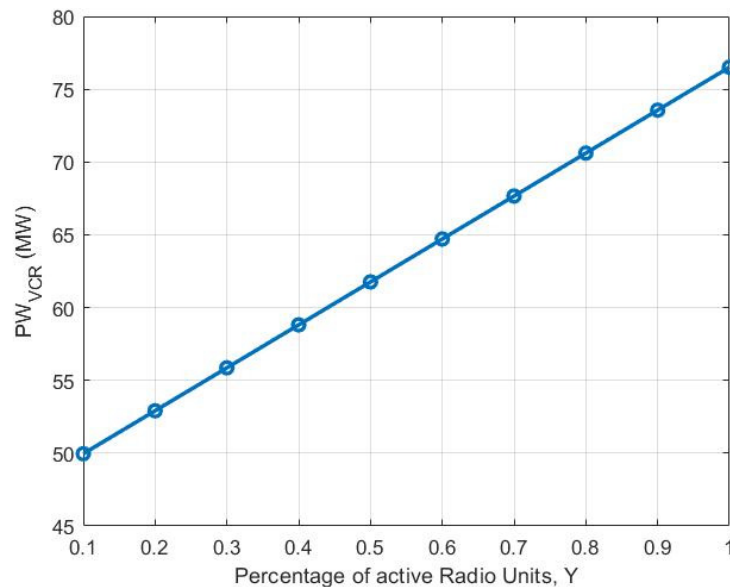
Figure 17. The variation in the overall power usage for VRAN 5G with active RUs.

In accordance with both the centralized and decentralized situations, Figure 17 illustrates that the overall power usage tends to increase linearly with the ratio of active RUs. However, for a similar number of active RUs, the centralized design required 84 MW of power, whereas the 5G Cloud C-RAN scenario used 71 MW. As a result, the total amount of power used is reduced by 15%. The latter observation further supports the claim that virtualizing the RAN results in a more efficient use of computer resources [4]. Figure 18

shows a bar chart that breaks down the 5G Cloud C-RAN network's total power consumption by section.
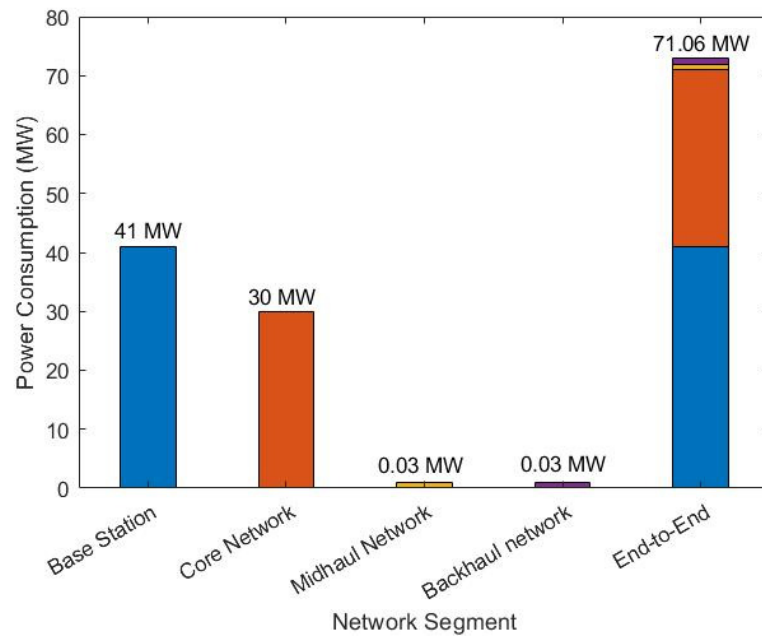
Figure 18. Power consumption breakdown for various network segments in the VRAN-based 5G network.

The end-to-end power consumption of the three 5G network architectures examined in this study—the virtualized 5G RAN scenario (PW_{VCR}), the centralized 5G architecture with hardware-based CU deployment (PW_{HCR}), and the 5G decentralized network scenario (PW_{DEC})—is depicted in Figure 19. The parameters taken into consideration are modified from the works of [4,8–10,12,13], and a comparison study has been conducted for the comparable ranges of active RUs.

Figure 19. Comparative analysis for PW_{DEC}, PW_{HCR}, and PW_{VCR}.

The comparison study incorporates typical values from [13,15], assuming an equal power consumption at the backhaul and core network levels for all three scenarios. 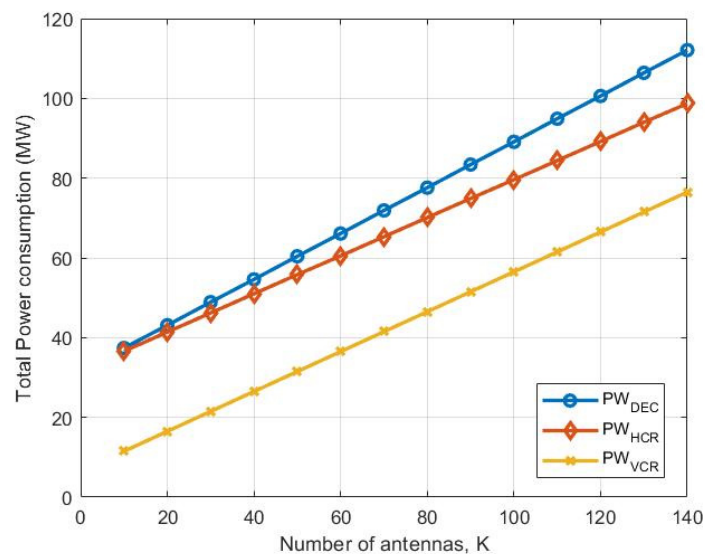This assumption is based on the use of PON technology in all three 5G models, which requires only a single OLT to connect all of the RRUs. Additionally, it is assumed that SDN architecture controllers optimize the traffic flow by utilizing all of the network elements to achieve an optimal latency–reliability compromise. Power models were developed for three different scenarios, with the number of active antennas or RUs being the primary dependent variable. As illustrated in Figure 20, the end-to-end power consumption for the three scenarios increased almost linearly with the number of active antennas. Furthermore, the power usage attributed to the BSs ranged from 41 MW to 65 MW, accounting for 58% to 68% of the total demand for the 5G network globally. These findings align with previous research indicating that base stations can account for up to 80% of the total power consumption in 5G networks [35].

The findings indicate that the 5G D-RAN architecture exhibits the highest power consumption among the three evaluated architectures: 5G D-RAN, 5G C-RAN, and 5G Cloud C-RAN. Specifically, the power consumption for the 5G D-RAN scenario was measured at 95 MW. In comparison, the 5G C-RAN scenario demonstrated a power consumption of 84 MW, which is approximately 12% lower than that of the 5G D-RAN. Previous studies, such as those by [44,45], have highlighted that 5G C-RANs can achieve a reduced power consumption through dynamic resource allocation and virtualization techniques. Furthermore, consistent with the findings of [10], the 5G Cloud C-RAN network was observed to consume significantly less power, at 71 MW, compared to both the 5G C-RAN (84 MW) and 5G D-RAN (95 MW) scenarios. This represents a reduction in power consumption of approximately 12% and 25%, respectively. Figure 20 illustrates the comparative end-to-end power consumption across the three 5G network topologies considered in this study. It is important to note that the analysis assumed 115 active antennas, as detailed in Section 4.1.
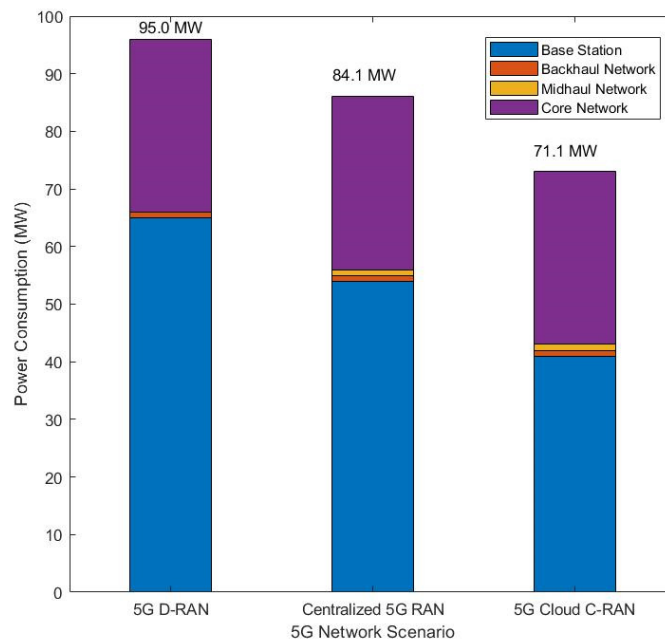

Figure 20. A comparison of the end-to-end power usage of 5G networks.

5. Perspectives on 6G RAN Architectures and Potential Power Models

Since there are currently no 3GPP standard specifications for the 6G RAN, a review of the RAN models being proposed for 6G is presented in this section. A few power models that could be used in 6G are also presented.

5.1. Proposed 6G RAN Architectures

The initial deployment of 6G technology is anticipated for 2027. However, numerous proposals for 6G RAN architectures have already been put forward. The white paper referenced in [46] offers valuable insights into the potential opportunities, benefits, and challenges associated with Open RAN architectures, including those for 6G networks. This research underscores the necessity of adopting innovative approaches to the design and implementation of mobile networks to meet the diverse requirements of future deployment strategies and usage models. According to [46], "open RAN" is characterized as a software-virtualized RAN comprising discrete components with open interface standards, such as open fronthaul. This approach, which leverages collaboratively developed open interfaces and standards, facilitates implementation on non-proprietary hardware and software. Furthermore, Open RAN enhances the network performance and user experience by integrating intelligence through open platforms based on artificial intelligence and machine learning.

The advent of 6G networks is expected to bring significant benefits through the adoption of open and disaggregated network designs. Firstly, these networks can be customized to meet the specific requirements of various use cases, thereby addressing the diverse needs of different applications. Open RAN exemplifies this approach by enhancing efficiency and scalability through the migration of network functions to the cloud. Additionally, the introduction of new interfaces alongside the existing 3GPP open interfaces, as proposed by Open RAN, can increase market flexibility and potentially boost competition within the telecommunications supply chains. By facilitating the reuse of multi-vendor network components and the integration of new elements to support 6G scenarios, open and disaggregated network architectures can significantly aid the transition to 6G [46].

Future mobile networks are expected to continue the trend of network horizontalization, which includes features such as hardware/software separation, management, and exposure. The advent of 6G presents an opportunity to re-evaluate and enhance the 3GPP-standardized functional architecture to better align with network horizontalization. An effective orchestration of the RAN and core networks is essential to harmonize infrastructure, administration, and tools, which have been key focus areas in the development of open RAN. In the 6G era, achieving network horizontalization involves several competitive architectural strategies, including cloudification and orchestration, the implementation of an open fronthaul interface to enable flexible RAN disaggregation, and the exposure of the network through new interfaces and control components derived from the current O-RAN design. To meet the increasing demand for ubiquitous connectivity across both societal and industrial sectors, 6G networks are designed to support a broader range of use cases. The drive towards a more open and intelligent network, while maintaining simplicity and sustainability, is guided by diverse criteria. Network horizontalization is viewed as the ongoing trend towards the convergence of previously isolated technology domains, such as telecommunications and IT, onto a unified service platform. Openness is anticipated to be a crucial element in the evolution of 6G, as it is vital for component and system interoperability, system efficiency, and service innovation.

Moreover, [46] asserts that energy efficiency and the reduction of the carbon footprint are central to the development of next-generation mobile networks. Despite a tenfold improvement in energy efficiency per bit, the transition to 5G has led to increased cell and antenna density, resulting in a tenfold rise in energy consumption. As 6G progresses

towards higher frequencies, such as Terahertz (THz), the challenge of energy consumption will intensify due to denser networks and smaller cells. Therefore, a significant reduction in energy consumption per bit is a key incentive for 6G solutions. These solutions offer several energy efficiency benefits, including system-on-chip technologies that produce less heat, power amplifiers with higher energy efficiency, innovative features like deep sleep software functionality (which can reduce the power consumption of mMIMO radios by up to 70% during off-peak hours), and the ability to switch traffic to the most energy-efficient bands. However, several challenges may arise with the implementation of an open RAN design. It is widely recognized that managing multiple vendors and open interfaces introduces security risks. Additionally, it can be complex to oversee the lifecycle, integrate various platforms (such as the RAN Intelligent Controller (RIC) and Service Management and Orchestration components), and ensure their seamless operation across different vertical use cases. Furthermore, the mix-and-match approach of the end-to-end (E2E) solution can be problematic due to the network's complexity, particularly in integrating components from various vendors. These factors could impede widespread compatibility among vendors.

The application of Artificial Intelligence (AI)-based Radio Access Networks (RAN) in the transition from 5G to 6G technology has been examined in [47], emphasizing aspects such as the planning and optimization of RF resources, network reach and capacity management, and use cases across various industries. Deep learning (DL), a subset of machine learning (ML), and AI are considered central to the innovative technologies of 6G. These technologies facilitate communications at multiple layers using millimeter wave (mmWave) and THz waves, and support channel detection and modulation categorization at the physical layer. Additionally, DL is utilized for channel assignment and beamforming design at the link layer. In mmWave and THz systems, channel estimation frequency and the associated overhead can increase significantly due to micro-range channel variations. AI-RAN systems can predict network traffic patterns, adjust network capacity, and reduce the need for over-provisioning. Furthermore, AI-RAN can optimize network resource allocation in real-time, ensuring an efficient distribution of resources to meet user demands. Intelligent automation and orchestration facilitated by AI-RAN can lead to better decision-making. AI aids the industry by automating routine network tasks and enhancing service delivery, allowing operators to focus on more strategic activities. Another feature enabled by AI-RAN is network slicing, which allows network operators to create virtualized network segments tailored to specific user needs. With AI, RAN networks can become more reliable, flexible, and efficient, while also reducing costs and improving decision-making.

The next generation of networks is anticipated to be significantly shaped by AI-RAN. Employing deep learning techniques to optimize network performance, predict traffic patterns, and efficiently allocate radio resources could greatly enhance 6G RF planning and optimization. AI methods can self-adjust parameters such as antenna tilting, beamforming, and power control by analyzing vast amounts of data, thereby improving signal quality, reducing interference, and increasing the overall network efficiency. Additionally, the coverage and capacity management of 6G AI-RAN networks can be dynamically adjusted in real-time to meet demand, ensuring an optimal service with minimal congestion. However, integrating AI-RAN architecture will require substantial computational power, efficient methodologies, and robust infrastructure to manage the increased complexity and processing demands [47]. In a similar research direction, the exploration of Open RAN's application of Artificial Intelligence has emerged as a promising field. Researchers have investigated methodologies and technologies to enable virtualization, network slicing, and multi-vendor interoperability while leveraging open-source software within Open RAN frameworks to enhance network performance, resource allocation, and

scalability. Open RAN advocates for open interfaces and software-defined networking to improve network flexibility, interoperability, and cost efficiency [48].

Integrating current terrestrial communication systems with aerial radio access networks (ARANs) represents a promising new direction. Utilizing satellites, drones, and unmanned aerial vehicles (UAVs), ARANs can rapidly establish a flexible access network on demand. As we advance towards a comprehensive 6G global access infrastructure, ARANs are expected to facilitate the development of efficient mobile communication systems. The framework proposed by researchers in [40] outlines the deployment of Aerial RANs over 6G networks. By employing aerial base stations (ABSs), ARANs provide end users with a radio access medium delivered from the sky for Internet services. Common examples of ABSs include UAVs, drones, balloons, and airplanes. Terrestrial macro base stations or miniaturized satellites can offer backhaul links. Future research is anticipated to benefit from a comprehensive and standardized reference model that integrates existing systems into a multitier and hierarchical ARAN.

An ARAN architecture typically consists of three main components: a primary segment that includes a cross-tier networking infrastructure shared among Aerial Base Stations (ABSs) at Low Altitude Platform (LAP), High Altitude Platform (HAP), and Low Earth Orbit (LEO) altitudes; a frontend interface that provides terrestrial and aerial access points to collect user connections; and a backend interface that connects the ARAN infrastructure to terrestrial core networks. Developing energy consumption models for aerial communications necessitates careful consideration of various factors, such as different types of UAVs, flight speeds, accelerations, payloads, and environmental conditions like weather. These factors are crucial because UAVs often operate in highly variable environments, which significantly affect their flight capabilities. For example, a UAV can achieve higher speeds with a lower energy consumption when flying with the wind. Additionally, ambient temperature can directly impact efficiency by affecting battery life [40].

5.2. Power Consumption in 6G Networks

The telecom sector is increasingly concerned with rising energy consumption, a trend that extends to 6G discussions, where the goal is to achieve continuous service growth while reducing network energy usage. In their report, [49] describe how the mobile industry is preparing to design the new 6G standard, which aims to provide even greater energy savings than 5G NR. As a new generation technology, 6G offers a unique opportunity to address the significant energy costs associated with cellular networks, with the RAN accounting for up to 76% of energy consumption. To create a more energy-efficient network, it is crucial to understand traffic characteristics and ensure that 6G can leverage deployment designs that centralize RAN operations to minimize energy usage. The radio product industry is also increasingly adopting a lower-layer split, which enhances RAN processing resource coordination, virtualization, adaptability, and hardware pooling, yielding substantial benefits. The lean architecture of 5G NR, which prioritizes data-related transmissions and eliminates unnecessary ones, has been highly effective, enabling networks to save considerable energy through micro-sleep.

Building on the successful implementations of lean design in 5G, it is prudent to extend these principles into 6G. Key considerations for 6G lean design include enhanced time-domain lean design, which involves further reducing the time-domain footprint of signals associated with idle mode, such as system information broadcasts, paging, and random access, and increasing the opportunities for micro-sleep transmission and reception in network equipment. Spatial domain lean design can limit system information transmission to a subset of transmission locations and utilize single-frequency-network (SFN) transmission formats to expand coverage. Frequency domain lean design focuses on improving solutions that enable carriers to operate without transmitting system

information, as the regular transmission of downlink mobility reference signals (RS) is not necessary for all of the carriers; only certain carriers need to support specific criteria and functions, allowing for a dynamic adjustment of the carrier capacity to meet current traffic demands.

The next 6G system presents a significant opportunity to enhance lean design improvements and ensure that all user devices support these features from the initial release. Achieving an energy-efficient network requires careful tuning based on real-time traffic and performance needs. The design must prioritize the scalability and rapid adaptation to maintain the optimal operation with the fewest active hardware components. Enhanced visibility into end-user experience and real-time network energy utilization enables a fast and precise hardware setup and management [49,50]. Similarly, [51] emphasized the critical need for sustainable energy solutions in future wireless networks as the number of connected devices and mobile terminals continues to grow. In response, 6G sustainable networks are rapidly emerging to provide energy-efficient solutions for connected networks.

A power optimization model for 6G-enabled massive IoT networks aimed at enhancing the system performance while minimizing the power overhead due to the large number of connected devices was developed in [51]. By optimizing power resource management, the proposed network was tested for the maximum power allocation and spectral efficiency across various network operations with different precoding schemes. Notably, cell-free networks are emerging as a highly promising technology for 6G communication scenarios. Cell-free massive MIMO is an innovative approach that employs a distributed network of access points (APs) to support a large number of users, with each AP serving a subset of users. The study proposed two user-scheduling algorithms to allocate users among the APs. The performance of the proposed model was evaluated for different precoding schemes, considering parametric variations in AP deployment, Channel State Information (CSI) availability, spatial correlation, and the number of antennas at the AP. It was found that APs with numerous antennas and a less dense deployment achieved better spectral efficiency.

For both maximal ratio (MR) and local minimum mean square error (LPMMSE) precoding, the network performance declines with a spatial correlation in distributed network operations when the access point (AP) manages all signal processing. With perfect channel state information (CSI), 95% of network users employing the partial minimum mean square error (PMMSE) precoding should experience a 4.1% improvement in spectral efficiency (SE). Additionally, the system's performance, incorporating power optimization mechanisms, was evaluated using the proposed user-scheduling methodologies. Each AP sets its maximum power at 141.7 mW for users with strong channels and its minimum power at 3.19 mW for users with weak channels using centralized PMMSE precoding. The Minimum Distance Scheduling (MCS) algorithm enhances the spectral efficiency for all users compared to the MDS algorithm. It was also observed that fractional power allocation achieves the optimal performance, providing most users with a higher spectral efficiency.

To mitigate the environmental impact and energy consumption of future cellular networks, it is crucial to explore network energy saving (NES) solutions as we advance towards 6G wireless technology. This technology promises ultra-high data rates, exceptionally low latency, and a substantial increase in the number of connected devices. The 3rd Generation Partnership Project (3GPP) has proposed the use of network-controlled repeaters (NCRs) to enhance the network coverage cost-effectively. In this context, [2] examines NES methods for future 6G networks and recommends optimal NES strategies aimed at maximizing the network's overall energy efficiency. As a cost-effective and energy-efficient approach to enhancing the performance of future 6G networks, repeaters

facilitate power reductions at next-generation nodeB (gNB) and improve both the overall energy efficiency (EE) and spectrum efficiency (SE).

The primary objective discussed in [2] was to optimize a set of parameters for next-generation nodeB (gNB) and network-controlled repeaters (NCR) to achieve the highest possible network energy efficiency (EE). The study measured the EE benefits and the associated spectral efficiency (SE) losses by examining trade-offs between the energy-efficient operation and quality of service (QoS) degradation for user equipment (UE). This was accomplished through an analytical study of basic network configurations with and without a repeater (or NCR), and a comprehensive simulation of the entire system to assess the effects of energy-efficient operations in a realistic network rollout. Recommendations were made to implement network energy saving (NES) and energy-efficient operations using various power amplifier (PA) technologies. The analysis considered two main scenarios: direct and indirect network topologies. The direct topology involved a direct connection between UE and gNB, with variable parameters at the gNB including the number of active antenna elements for transmission, their respective PA output power, and bandwidth, while the number of receiving antennas for the UE was assumed to be fixed. In the indirect scenario, an NCR was used to connect the UE to the gNB. For evaluating the system's energy efficiency, the NCR's parameters, such as the proportion of antennas involved in transmission and reception processes, along with the gNB's settings, were considered.

The power consumption model presented for the gNB and network-controlled repeaters (NCRs) is detailed below.

$$PW_{gNB}(DLK) = PW_{fx,gNB} + \propto \times PW_{notPA} + \emptyset \times PW_{PA} \tag{18}$$

where $PW_{fx,gNB}$ is the constant power consumption component that does not vary with gNB settings, PW_{notPA} is the power consumption not related to the power amplifier and varies according to the number of radio units deployed, PW_{PA} is the power consumption of power amplifiers, and the power consumption of power amplifiers is calculated as follows:

$$\frac{NA_{Txn,gNB} \times PAop_{gNB}}{StdTxPW_{RU}} \times \frac{1}{\eta} \times (PW_{act,DL} - PW_{fx,gNB}) \tag{19}$$

where $NA_{Txn,gNB}$ is the number of antenna elements actively involved in transmission, $PAop_{gNB}$ is the power amplifier output power of every antenna element, and $StdTxPW_{RU}$ is the standard transmit power of each radio unit. η is the normalized power amplifier efficiency, and $PW_{act,DL}$ is the reference value, and $PW_{fx,gNB}$ is the constant power consumption component that does not vary with gNB settings.

The power consumption of the network-controlled repeater is calculated as follows:

$$PW_{NCR}(DLK) = PW_{fx,NCR} + PW_{rcv,NCR} + PW_{trx,NCR} \tag{20}$$

where $PW_{fx,NCR}$ is the standard component related to the network-controlled functions of the NCR, $PW_{rcv,NCR}$ is the power consumed by the analogue receive front-end of NCR, and $PW_{trx,NCR}$ is the power consumed by the analogue transmit front-end of NCR.

The simulations were conducted using a 28 GHz band with 400 MHz of the operating bandwidth, assuming a fully loaded gNB and 100% buffer traffic. In the link-level direct topology scenario, energy efficiency improved by approximately 30%, albeit with a rate degradation of up to 10%. Conversely, varying the power amplifier efficiency resulted in a 60% improvement in energy efficiency, accompanied by a 20% decrease in spectral efficiency. For the indirect topology scenario, simulations revealed a 56% increase in energy efficiency, with a rate performance drop ranging from 3% to 20% when the energy efficiency optimization algorithms were applied. Ref. [2] demonstrated that NES techniques could be employed to adjust the transmit and receive the parameters of gNB and NCR, enhancing energy efficiency (EE) and reducing network power consumption. According

to our link and system-level findings, it is more energy-efficient in high SNR regimes to prioritize energy efficiency over spectral efficiency. Incorporating bias judgment and advanced power amplifier technology significantly improved energy efficiency compared to outdated power amplifier technologies. Additionally, networks utilizing repeaters benefited from enhanced spectral efficiency and contributed to power savings in gNB by leveraging the robust backhaul link, leading to a higher overall energy efficiency. Therefore, repeaters represent a cost-effective and energy-efficient approach to enhancing the future 6G network capacity and coverage.

6. Conclusions

5G is seen as a highly promising technology due to its improved mobile capacity, extremely reliable low latency, and sufficient support for MTC (machine-type communications). When contrasted with previous generations of mobile technology, the power consumption of 5G networks has grown tremendously. The 5G networks' requirement for denser mobile equipment has been the primary cause of this rise in power requirement [52]. For 5G technology to be financially and environmentally sustainable, improving energy efficiency is primordial. This study establishes a comprehensive framework for achieving the critical goal of optimizing the end-to-end power consumption in 5G networks. It analyzes the power usage of various components across different network segments in three primary deployment scenarios of 5G technology: 5G D-RAN with mMIMO technology, 5G C-RAN with dedicated physical hardware (similar to 5G Cloud D-RAN), and 5G Cloud C-RAN with virtualized DUs and CUs.

A detailed comparative analysis was performed for these three topologies using the available power ratings of different 5G RAN components and typical values from the existing literature. The study assumes the application of NGPON/GPON and SDN technologies in the backhaul and core network segments, respectively. It was found that the number of active radio units (antennae) significantly impacts end-to-end power consumption. The study demonstrated that the power consumption for the three architectures increases almost linearly with the number of active antennae. Among the scenarios, 5G D-RAN was identified as the highest power consumer. The study also confirmed that BSs are the largest power-consuming components within the 5G network, with power consumption ranging from 41 MW to 65 MW across the three models. This accounts for 58% to 68% of the global 5G network consumption. The 5G C-RAN scenario showed an approximately 12% lower power consumption than the 5G D-RAN scenario due to the dynamic allocation of computational resources. Additionally, the virtualized RAN 5G scenario consumed up to 25% less power than the decentralized architecture, attributed to the enhanced and dynamic resource allocation based on traffic requirements. However, it requires an additional mid-haul bandwidth between virtual CUs and DUs to ensure the required data rates are met.

Future research should focus on developing energy efficiency metrics to devise optimization strategies at different network segments, particularly at the Base Station level, which consumes the most energy. Furthermore, real-life data sets could be used with machine learning techniques to develop and implement optimization strategies, unlocking the vast potential of 5G technology across various industries. We believe that the 5G power model proposed in Sections 3 and 4 can potentially be used as a framework to develop a power model for 6G. Moreover, this model can also be relevant for initial 6G RAN architectures which are projected to be backward compatible with 5G and operate in tandem.

List of Symbols

Symbol	Meaning
BW_{S_i}	The capacity of the transport network required at the i-th BS considering the functional split
F_{CS}	The function split from the cloud site for the 5G Cloud C-RAN architecture
N_{BS}	The number of Base Stations in the network
$N_{OLT\ Cards}$	The total number of OLT cards
N_{OLT}	The ratio $[\frac{N_{ONT}}{N_{Splitter\ Ports}\ N_{OLT\ Cards}}]$,
N_{ONT}	The total number of ONTs being used in the network
N_{RU}	The sum of RUs in the network for the 5G Cloud C-RAN architecture
N_{SFP+}	The total number of SFPs installed within the network
$N_{Splitter\ Ports}$	The total quantity of splitter ports utilized to establish the necessary connections for ONTs
N_f	The number of wavelengths per fibre in the transport network
PW_{CO_i}	The proportion of the cooling power usage related to the i-th DU in the 5G Centralized scenario
PW_{DU_i}	The power consumed by the i-th implemented DU in 5G Centralized scenario
PW_{MH_i}	The power used by the i-th mid-haul link in the 5G Centralized scenario
PW_{NF_i}	The network functions' proportion of the power usage of shifted to the CU in the 5G Centralized scenario
PW_A	The active mode power consumption of the RUs for the 5G Cloud C-RAN architecture
PW_{CP}^{li}	The power consumed in the circuit, independent of load
PW_{CU}	The power usage of the BBU host where the CU is situated in the 5G Centralized scenario
PW_{HCR}	The end-to-end power consumption for 5G Centralized RAN architecture
PW_{Lk}	The links' power consumption for the 5G Cloud C-RAN architecture
PW_{ONT}	The power consumed by an ONT
PW_{RAN}	The power consumption of the Radio Access Network segment in the 5G Centralized scenario
PW_{RU}	The power attributed to an RU
PW_S	The sleep mode power consumption of the RUs for the 5G Cloud C-RAN architecture
PW_{SDN}	The sum of the power usage of the various elements that make up the SDN architecture in 5G Core Network

PW_{SFP+}	The power consumed by each of the SFPs.
PW_{VRAN}	The end-to-end power consumption for the 5G Cloud C-RAN architecture
PW_{add}	The additional power usage in BBU due to resource pooling in the 5G Centralized scenario
PW_{am}^{max}	The upper threshold for the power amplifier's power for the 5G Cloud C-RAN architecture
PW_{fx}	The constant power usage in each RU for the 5G Cloud C-RAN architecture
PW_{tx}	The transport network node's power usage
PW_{xc}	The power consumed by ports that cross connect on the transport network
R_{tx}	The rate of the transport network in Gbps pertaining to mid-haul links
Y_{UD}	The mean quantity of user devices (UDs) connected to each RU
$\propto$	The factor for direct current to radio frequency conversion
A	The aggregation of the power consumption needed by the coding/decoding operations and part of backhaul network that is independent of load, per bit of information
Ga_{CO}	The cooling gain
Ga_{pot}	The pooling gain
Ga_{st}	The stacking gain
K	The quantity of user equipment (UEs) that are in active mode
L	The packets queued in 5G Core Network due to latency
N	The quantity of antennae deployed at the Base Station
n	The total number of network elements, including switches, controllers, and latency queues in 5G Core Network
PW_{BL}	Backhaul network power consumption
PW_{BS}	Base Station power consumption
PW_{cj}	The power consumption of the controllers in 5G Core Network
PW_{DEC}	The end-to-end power consumption for 5G Decentralized RAN architecture
PW_{Elk}	The power consumed by the ethernet links in 5G Core Network
PW_{sj}	The power consumption of the switches in 5G Core Network
PW_{UE}	UE output power (downlink)
R_{UE}	The throughput of the UE
X_3	The beamforming processing component that has a linear variation with K^3
Y	The proportion of active RUs expressed as a percentage for the 5G Cloud C-RAN architecture
Y_0	The power consumed by each transceiver module that is connected to all antennae
Y_1	The beamforming processing component that has a linear variation with N.K
Y_2	The aggregation of the contributions of the beamforming processing and channel estimation and that has a linear variation with $N.K^2$
$z_1, z_2,$ and z_3	Constants derived from simulation based on the policy decisions of the SDN controller
ηPA	The power amplifier efficiency

List of Acronyms

Acronym (alphabetical)	Meaning
3GPP	Third Generation Partnership Project
4G	4th Generation
5G	5th Generation
5G NR	5G New Radio
6G	6th Generation

AAU	Active Antenna Unit
ABSs	Aerial Base Stations
AI	Artificial Intelligence
ANN	Artificial Neural Network
AP	Access Point
ARAN	Aerial Radio Access Networks
BBU	Base band Unit
BS	Base Station
CCS	Central Cloud Site
CPRI	Common Public Radio Interface
CPU	Central Processing Unit
C-RAN	Centralized Radion Access Network
CSI	Channel State Information
CU	Centralized Unit
D-RAN	Decentralized Radio Access Network
DU	Distributed Unit
eCPRI	Enhanced Common Public Radio Interface
EE	Energy Efficiency
eMBB	enhanced mobile broadband
Fronthaul-HL	front-haul-high layer
Front-haul-LL	front-haul-low layer
FTTH	Fibre-To-The-Home
GE	Giga Ethernet
GPON	Gigabit Passive Optical Network
HAP	High Altitude Platform
HetNets	Heterogeneous Networks
IoT	Internet of Things
ITU	International Telecommunications Union
LAP	Low Altitude Platform
LEO	Low Earth Orbit
LPMMSE	Local Minimum Mean Square Error
LTE	Long-Term Evolution
MAC	Media Access Control
MCS	Minimum Distance Scheduling
MDS	Multidimensional scaling
ML	Machine Learning
mMIMO	massive multiple-input multiple-output
mMTC	massive machine-type communication
mmW	millimeter wave
MR	Maximal Ratio
NCR	Network-Controlled Repeater

NES	Network Energy Saving
NGPON	Next Generation Passive Optical Network
OLT	Optical Line Terminal
ONT	Optical Network Terminal
PA	Power Amplifier
PDCP	Packet Data Convergence Protocol
PHY	Physical
PMMSE	Partial Minimum Mean Square Error
PoF	Power over Fibre
QoS	Quality of Service
RAN	Radio Access Network
RF	Radio Frequency
RIC	Radio Access Network Intelligent Controller
RLC	Radio Link Control
RRC	Radio Resource Control
RU	Radio Unit
SDAP	Service Data Adaptation Protocol
SDN	Software Defined Networking
SE	Spectral Efficiency
SFN	single-frequency-network
SFP	small form-factor pluggable module
UAV	Unmanned Aerial Vehicle
UE	User Equipment
uRLLC	ultra-reliable low-latency communications
vCUs	virtualized Centralized Units
vDUs	virtualized Distributed Units
VRAN	Virtualized Radio Access Network

References

1. Pana; V.S.; Babalola; O.P.; Balyan, V. 5G radio access networks: A survey. *Array* **2022**, *14*, 100170. https://doi.org/10.1016/j.array.2022.100170.
2. Azzino; T.; HasanzadeZonuzy; A.; Luo; J.; Abedini; N.; Luo, T. Towards Energy- and Cost-Efficient 6G Networks. *arXiv* **2024**, arXiv:2409.19121. https://doi.org/10.48550/arxiv.2409.19121.
3. Abrol, A.; Jha, R.K. Power Optimization in 5G Networks: A Step Towards GrEEn Communication. *IEEE Access* **2016**, *4*, 1355–1374. https://doi.org/10.1109/access.2016.2549641.
4. Lopez-Perez, D.; De Domenico, A.; Piovesan, N.; Xinli, G.; Bao, H.; Qitao, S.; Debbah, M. A Survey on 5G Radio Access Network Energy Efficiency: Massive MIMO, Lean Carrier Design, Sleep Modes, and Machine Learning. *IEEE Commun. Surv. Tutorials* **2022**, *24*, 653–697. https://doi.org/10.1109/comst.2022.3142532.
5. Gruber; M.; Blume; O.; Ferling; D.; Zeller; D.; Imran; M.A.; Strinati; E.C. EARTH—Energy Aware Radio and Network Technologies. In Proceedings of the 2009 IEEE 20th International Symposium on Personal, Indoor and Mobile Radio Communications, Tokyo, Japan, 13–16 September 2009. https://doi.org/10.1109/pimrc.2009.5449938.
6. Han, F.; Zhao, S.; Zhang, L.; Wu, J. Survey of Strategies for Switching Off Base Stations in Heterogeneous Networks for Greener 5G Systems. *IEEE Access* **2016**, *4*, 4959–4973. https://doi.org/10.1109/access.2016.2598813.

7. Poirot, V.; Ericson, M.; Nordberg, M.; Andersson, K. Energy efficient multi-connectivity algorithms for ultra-dense 5G networks. *Wirel. Networks* **2019**, *26*, 2207–2222. https://doi.org/10.1007/s11276-019-02056-w.

8. Piovesan, N.; Lopez-Perez, D.; De Domenico, A.; Geng, X.; Bao, H.; Debbah, M. Machine Learning and Analytical Power Consumption Models for 5G Base Stations *IEEE Commun. Mag.* **2022**, *60*, 56–62. https://doi.org/10.1109/mcom.001.2200023.

9. Hossain, M.M.A.; Cavdar, C.; Bjornson, E.; Jantti, R. Energy Saving Game for Massive MIMO: Coping With Daily Load Variation. *IEEE Trans. Veh. Technol.* **2017**, *67*, 2301–2313. https://doi.org/10.1109/tvt.2017.2769163.

10. Ismail, T.; Mahmoud, H.H.M. Optimum Functional Splits for Optimizing Energy Consumption in V-RAN. *IEEE Access* **2020**, *8*, 194333–194341. https://doi.org/10.1109/access.2020.3033879.

11. Moosavi, R.; Parsaeefard, S.; Maddah-Ali, M.A.; Shah-Mansouri, V.; Khalaj, B.H.; Bennis, M. Energy efficiency through joint routing and function placement in different modes of SDN/NFV networks. *Comput. Networks* **2021**, *200*, 108492. https://doi.org/10.1016/j.comnet.2021.108492.

12. Assefa, B.G.; Ozkasap, O. A survey of energy efficiency in SDN: Software-based methods and optimization models. *J. Netw. Comput. Appl.* **2019**, *137*, 127–143. https://doi.org/10.1016/j.jnca.2019.04.001.

13. Priyadarsini; Bera, P.; Rahman, M.A. A new approach for energy efficiency in software defined network. In Proceedings of the 2018 Fifth International Conference on Software Defined Systems (SDS), Barcelona, Spain, 23–26 April 2018. https://doi.org/10.1109/sds.2018.8370424.

14. Sharma, D.; Singhal, S.; Rai, A.; Singh, A. Analysis of power consumption in standalone 5G network and enhancement in energy efficiency using a novel routing protocol. *Sustain. Energy Grids Netw.* **2021**, *26*, 100427. https://doi.org/10.1016/j.segan.2020.100427.

15. Farias, F.; Fiorani, M.; Tombaz, S.; Mahloo, M.; Wosinska, L.; Costa, J.C.W.A.; Monti, P. Cost- and energy-efficient backhaul options for heterogeneous mobile network deployments. *Photon-Netw. Commun.* **2016**, *32*, 422–437. https://doi.org/10.1007/s11107-016-0676-6.

16. Abdelnaby, E.; Abd-Alaaty, H.; Nashat, M.; abd-elazim, M. Based on 6G, Fog Radio Access Network Behaviour Analysis. *Res. Sq.* **2024**. https://doi.org/10.21203/rs.3.rs-4101544/v1.

17. Vázquez, C.; Otero, G.; Altuna, R.; López-Cardona, J.D.; Larrabeiti, D. Power over Fiber Pooling as Part of 6G Optical Fronthaul. *J. Light. Technol.* **2024**, *42*, 4774–4781. https://doi.org/10.1109/jlt.2024.3375972.

18. Pfeiffer, T. Next Generation Mobile Fronthaul and Midhaul Architectures [Invited]. *J. Opt. Commun. Netw.* **2015**, *7*, B38–B45. https://doi.org/10.1364/jocn.7.000b38.

19. Mocerino, J. Paper—5G Backhaul/Fronthaul Opportunities and Challenges—NCTA Technical Papers. 2019. Available online: https://www.nctatechnicalpapers.com/Paper/2019/2019-5g-backhaul-fronthaul-opportunities-and-challenges (accessed on 21 September 2024).

20. Khatri, P. The Impact of 5G on IP Transport Networks. Available online: https://blog.apnic.net/2019/11/13/the-impact-of-5g-on-ip-transport-networks (accessed on 23 September 2024).

21. Moshin, M.; Batalla, J.M.; Pallis, E.; Mastorakis, G.; Markakis, E.K.; Mavromoustakis, C.X. On Analyzing Beamforming Implementation in O-RAN 5G. *Electronics* **2021**, *10*, 2162. https://doi.org/10.3390/electronics10172162.

22. Costa-Perez, X.; Garcia-Saavedra, A.; Li, X.; Deiss, T.; de la Oliva, A.; di Giglio, A.; Iovanna, P.; Moored, A. 5G-Crosshaul: An SDN/NFV Integrated Fronthaul/Backhaul Transport Network Architecture. *IEEE Wirel. Commun.* **2017**, *24*, 38–45. https://doi.org/10.1109/mwc.2017.1600181wc.

23. Zola, A.; Bernstein, C. What is Fronthaul? Available online: https://www.techtarget.com/searchmobilecomputing/definition/fronthaul (accessed on 1 April 2024).

24. de Oliveira, W.; Batista, J.O.R.; Novais, T.; Takashima, S.T.; Stange, L.R.; Martucci, M.; Cugnasca, C.E.; Bressan, G. OpenCare5G: O-RAN in Private Network for Digital Health Applications. *Sensors* **2023**, *23*, 1047. https://doi.org/10.3390/s23021047.

25. Tabbane, S. 5G Networks and 3GPP Release 15. 2019. Available online: https://www.itu.int/en/ITU-D/Regional-Presence/AsiaPacific/SiteAssets/Pages/Events/2019/ITUPITA2018/ITU-ASP-CoE-Training-on-/5G%20networks%20and%203GPP%20Release%2015_vf.pdf (accessed on 15 July 2024).

26. Pietilä, A.-K.; Marshall, P. Tap into the Next Big Thing with Cloud RAN|Nokia. 2021. Available online: https://www.nokia.com/blog/tap-into-the-next-big-thing-with-cloud-ran/ (accessed on 15 March 2023).

27. Lee, M. An Introduction to 5G New Radio Architecture|Electronics360. 2022. Available online: https://electronics360.globalspec.com/article/18374/an-introduction-to-5g-new-radio-architecture (accessed on 24 November 2024).

28. Lavallee, B. Spotlight on 4G/5G Backhaul Networks. 2022. Available online: https://www.ciena.com/insights/articles/spotlight-on-4g-5g-backhaul-networks.html?utm_source=Blog&utm_medium=Social (accessed on 24 November 2024).

29. Giannopoulos, A.; Spantideas, S.; Kapsalis, N.; Karkazis, P.; Trakadas, P. Deep Reinforcement Learning for Energy-Efficient Multi-Channel Transmissions in 5G Cognitive HetNets: Centralized, Decentralized and Transfer Learning Based Solutions. *IEEE Access* **2021**, *9*, 129358–129374. https://doi.org/10.1109/access.2021.3113501.

30. Cai, S.; Che, Y.; Duan, L.; Wang, J.; Zhou, S.; Zhang, R. Green 5G Heterogeneous Networks Through Dynamic Small-Cell Operation. *IEEE J. Sel. Areas Commun.* **2016**, *34*, 1103–1115. https://doi.org/10.1109/jsac.2016.2520217.

31. Meng, F.-X.; Chen, P.; Wu, L. Power Allocation in Multi-User Cellular Networks with Deep Q Learning Approach. In Proceedings of the ICC 2019—2019 IEEE International Conference on Communications (ICC), Shanghai, China, 20–24 May 2019. https://doi.org/10.1109/icc.2019.8761431.

32. Lenderman, J.; Kunstler, J.; Wilson, S., "2024 Trends to Watch: Broadband Access," Omdia, England, Sep. 2024. Accessed on 10 August 2024. [Online]. Available: https://omdia.tech.informa.com/om033878/2024-trends-to-watch-broadband-access

33. Carapellese, N.; Pizzinat, A.; Tornatore, M.; Chanclou, P.; Gosselin, S. An energy consumption comparison of different mobile backhaul and fronthaul optical access architectures. In Proceedings of the 2014 The European Conference on Optical Communication (ECOC), Cannes, France, 21–25 September 2014. https://doi.org/10.1109/ECOC.2014.6964023.

34. Fiorani, M.; Tombaz, S.; Mårtensson, J.; Skubic, B.; Wosinska, L.; Monti, P. Modeling Energy Performance of C-RAN With Optical Transport in 5G Network Scenarios *J. Opt. Commun. Netw.* **2016**, *8*, B21–B34. https://doi.org/10.1364/jocn.8.000b21.

35. Mughees, A.; Tahir, M.; Sheikh, M.A.; Ahad, A. Towards Energy Efficient 5G Networks Using Machine Learning: Taxonomy, Research Challenges, and Future Research Directions. *IEEE Access* **2020**, *8*, 187498–187522. https://doi.org/10.1109/access.2020.3029903.

36. Abdulghaffar, A.; Mahmoud, A.; Abu-Amara, M.; Sheltami, T. Modeling and Evaluation of Software Defined Networking Based 5G Core Network Architecture. *IEEE Access* **2021**, *9*, 10179–10198. https://doi.org/10.1109/access.2021.3049945.

37. Jaffer, S.S.; Hussain, A.; Qureshi, M.A.; Khan, Y.; Mirza, J.; Qureshi, K.K.; Ali, M.M. Reliable and cost-efficient protection scheme for 5G fronthaul/backhaul network. *Heliyon* **2023**, *9*, e14215. https://doi.org/10.1016/j.heliyon.2023.e14215.

38. Hantoro, G.D. GPON Performance Analysis for 5G Backhaul Solutions. In Proceedings of the TENCON 2018—2018 IEEE Region 10 Conference, Jeju, Republic of Korea, 28–31 October 2018. https://doi.org/10.1109/TENCON.2018.8650520.

39. Sigwele, T.; Alam, A.S.; Pillai, P.; Hu, Y.F. Energy-efficient cloud radio access networks by cloud based workload consolidation for 5G. *J. Netw. Comput. Appl.* **2017**, *78*, 1–8. https://doi.org/10.1016/j.jnca.2016.11.005.

40. de Alwis, C.; Pham, Q.-V.; Liyanage, M. 6G Radio Access Networks, In *6G Frontiers: Towards Future Wireless Systems*; John Wiley & Sons, Inc.: Hoboken, NJ, USA, 2022; pp. 99–114. https://doi.org/10.1002/9781119862321.ch9.

41. Bjornson, E.; Sanguinetti, L.; Hoydis, J.; Debbah, M. Optimal Design of Energy-Efficient Multi-User MIMO Systems: Is Massive MIMO the Answer? *IEEE Trans. Wirel. Commun.* **2015**, *14*, 3059–3075. https://doi.org/10.1109/twc.2015.2400437.

42. Syed-Yusof, S.K.; Numan, P.E.; Yusof, K.M.; Din, J.B.; Marsono, M.N.B.; Onumanyi, A.J. Software-Defined Networking (SDN) and 5G Network: The Role of Controller Placement for Scalable Control Plane. In Proceedings of the 2020 IEEE International RF and Microwave Conference (RFM). Kuala Lumpur, Malaysia, 14–16 December 2020. https://doi.org/10.1109/RFM50841.2020.9344741.

43. Cavaliere, F.; Dahlfort, S.; Tartaglia, A.; Bergström, J.; Tavemark, A.; Åkerström, P.; Sinicrope, D. Optimized Optical Solutions for Mobile Transport Networks. ERICSSON. 2022. Available online: https://www.ericsson.com/494925/assets/local/reports-papers/white-papers/optimized-optical-solutions-for-mobile-transport-networks.pdf (accessed on 18 May 2023).

44. Andersson, C.; Bengtsson, J.; Byström, G.; Frenger, P.; Jading, Y.; Nordenström, M. Improving Energy Performance in 5G Networks and Beyond. ericsson.com. 2023. https://www.ericsson.com/en/reports-and-papers/ericsson-technology-review/articles/improving-energy-performance-in-5g-networks-and-beyond (accessed on 16 July 2024).

45. Wang, X.; Alabbasi, A.; Cavdar, C. Interplay of energy and bandwidth consumption in CRAN with optimal function split. In Proceedings of the IEEE International Conference on Communications (ICC), Paris, France, 21–25 May 2017. https://doi.org/10.1109/ICC.2017.7997127.

46. Erkens, H.; Mildh, G.; Hoymann, C.; Summer, R.; Garcia, G. Open Ran and 6G Future Networks Development. [Online] 6G-IA. Europe: 6G Smart Networks and Services Industry Association. 2024. Available online: https://6g-ia.eu/wp-content/uploads/2024/05/6g-ia-open-sns_open-networks-status-and-future-development_ran-final.pdf (accessed on 12 November 2024).

47. Khan, N.A.; Schmid, S. AI-RAN in 6G Networks: State-of-the-Art and Challenges. *IEEE Open J. Commun. Soc.* **2023**, *5*, 294–311. https://doi.org/10.1109/ojcoms.2023.3343069.

48. Choi, A. AI-Native Open RAN for 6G. O-RAN Alliance. 2023. Available online: https://www.itu.int/en/ITU-T/Workshops-and-Seminars/2023/0724/Documents/AlexChoi.pdf (accessed on 20 November 2024).

49. Frenger, P.; Jading, Y.; Nader, A. Energy Performance of 6G Radio Access Networks: A Once in a Decade Opportunity. Ericsson. 2024. Available online: https://www.ericsson.com/en/reports-and-papers/white-papers/energy-performance-of-6g-ran (accessed on 20 November 2024).

50. Tombaz, S.; Frenger, P.; Athley, F.; Semaan, E.; Tidestav, C.; Furuskar, A. Energy Performance of 5G-NX Wireless Access Utilizing Massive Beamforming and an Ultra-Lean System Design. In Proceedings of the 2015 IEEE Global Communications Conference (GLOBECOM), San Diego, CA, USA, 6–10 December 2015. https://doi.org/10.1109/glocom.2014.7417240.

51. Taneja, A.; Saluja, N.; Taneja, N.; Alqahtani, A.; Elmagzoub, M.A.; Shaikh, A.; Koundal, D. Power Optimization Model for Energy Sustainability in 6G Wireless Networks. *Sustainability* **2022**, *14*, 7310. https://doi.org/10.3390/su14127310.

52. Sethi, J.; Fan, Y.; Ehrnborg, G. Elevating 5G with Differentiated Connectivity. Available online: https://www.ericsson.com/en/reports-and-papers/consumerlab/reports/elevating-5g-with-differentiated-connectivity (accessed on 24 November 2024).